

DESY 99-083
 UdeM-GPP-TH-99-60
 May 1999

PRECISION FLAVOUR PHYSICS AND SUPERSYMMETRY [★]

Ahmed Ali

Deutsches Elektronen-Synchrotron DESY, Hamburg, Germany

David London

*Laboratoire René J.-A. Lévesque, Université de Montréal,
 C.P. 6128, succ. centre-ville, Montréal, QC, Canada H3C 3J7*

Abstract

We review the salient features of a comparative study of the profile of the CKM unitarity triangle, and the resulting CP-violating phases α , β and γ in B decays, in the standard model and in several variants of the minimal supersymmetric standard model (MSSM), reported recently by us. These theories are characterized by a single phase in the quark flavour mixing matrix and give rise to well-defined contributions in the flavour-changing-neutral-current transitions in K and B decays. We analyse the supersymmetric contributions to the mass differences in the B_d^0 - \overline{B}_d^0 and B_s^0 - \overline{B}_s^0 systems, ΔM_d and ΔM_s , respectively, and to the CP-violating quantity $|\epsilon|$ in K decays. Our analysis shows that the predicted ranges of β in the standard model and in MSSM models are very similar. However, precise measurements at B -factories and hadron machines may be able to distinguish these theories in terms of the other two CP-violating phases α and γ .

[★] Contribution to the Festschrift for L. B. Okun, to appear in a special issue of Physics Reports, eds. V. L. Telegdi and K. Winter

1 Introduction

In this article, written to honour the scientific achievements of Lev Okun, we discuss some selected topics in quark flavour physics. In particular, we review the present status of quark flavour mixing in the Standard Model (SM) and in some variants of the Minimal Supersymmetric Standard Model (MSSM). The idea is to present contrasting profiles of quark flavour physics in these theoretical frameworks which can be tested in the next generation of experiments in flavour physics. The emphasis in this paper is on CP violating asymmetries and particle-antiparticle mixings induced by weak interactions. These topics are close to Lev Okun's own scientific research. In fact, the possibility of observing violation of CP-invariance in heavy particle decays was proposed in an important paper by Okun, Pontecorvo and Zakharov in 1975, just after the discovery of the charmed hadrons [1]. To be specific, these authors studied the consequences of $D^0\overline{D}^0$ pair production, subsequent $D^0\text{-}\overline{D}^0$ mixing, and CP violation for the final states involving same-sign $\ell^\pm\ell^\pm$ and opposite-sign $\ell^+\ell^-$ dileptons. In particular, as a measure of $D^0\text{-}\overline{D}^0$ mixing they proposed the measurement of the ratio of the same-sign to the inclusive dilepton events,

$$R_D \equiv \frac{N^{++} + N^{--}}{N^{+-} + N^{-+} + N^{++} + N^{--}} = \frac{1}{2} \frac{(\Gamma_S - \Gamma_L)^2 + 4(\Delta M_{SL})^2}{(\Gamma_S + \Gamma_L)^2 + 4(\Delta M_{SL})^2} , \quad (1)$$

where Γ_S and Γ_L are the widths of the (short-lived) D_S and (long-lived) D_L mesons, respectively, and ΔM_{SL} is their mass difference. They also suggested the measurement of the charge asymmetry

$$\delta_D \equiv \frac{N^{++} - N^{--}}{N^{++} + N^{--}} \simeq 4\text{Re } \epsilon_D , \quad (2)$$

as a measure of CP violation. Here, ϵ_D is the CP-violating parameter in the wave-functions of D_S and D_L mesons, analogous to the corresponding parameter ϵ_K in the K -system [2],

$$D_S \sim D_1 + \epsilon_D D_2, \quad D_L \sim D_2 + \epsilon_D D_1 , \quad (3)$$

where D_1 and D_2 are the pure CP states.

So far, neither R_D nor δ_D have been measured [2]. In fact, in the Cabibbo-Kobayashi-Maskawa (CKM) theory of quark flavour mixing [3], which is now an integral part of the SM, no measurable effects are foreseen for either of the ratios R_D and δ_D , due to the experimentally established hierarchies in the quark mass spectrum and the CKM matrix elements. Typically, one has in

the SM [4],

$$\frac{\Delta M_{SL}}{\Gamma_S + \Gamma_L} \simeq O(10^{-5}), \quad \frac{\Gamma_S - \Gamma_L}{\Gamma_S + \Gamma_L} \ll 1, \quad (4)$$

with δ_D completely negligible. By virtue of this, the quantities R_D and δ_D have come to be recognized as useful tools to search for physics beyond the SM [5,6].

The OPZ formulae also apply to the time-integrated effects of mixing and CP violation in the $B_d^0-\overline{B}_d^0$ and $B_s^0-\overline{B}_s^0$ systems, and they were used in the analysis [7] of the UA1 data on inclusive dilepton production [8]. Calling the corresponding mixing measures R_{B_d} and R_{B_s} , respectively, present experiments yield $R_{B_d} \simeq 0.17$ and $R_{B_s} \simeq 1/2$ [2]. These measurements are consistent with the more precise time-dependent measurements, yielding $\Delta M_{B_d} = 0.471 \pm 0.016 \text{ (ps)}^{-1}$ [9] and the 95% C.L. upper limit $\Delta M_{B_s} > 12.4 \text{ (ps)}^{-1}$ [10]. However, the corresponding CP-violating charge asymmetries δ_{B_d} and δ_{B_s} in the two neutral B -meson systems have not been measured, with the present best experimental limit being $\delta_{B_d} = 0.002 \pm 0.007 \pm 0.003$ from the OPAL collaboration [2] and no useful limit for the quantity δ_{B_s} . These charge asymmetries are expected to be very small in the SM, reflecting essentially that the width and mass differences $\Delta\Gamma$ and ΔM in the $B_d^0-\overline{B}_d^0$ and $B_s^0-\overline{B}_s^0$ complexes are relatively real. Typical estimates in the SM are in the range $\delta_{B_d} = O(10^{-3})$ and $\delta_{B_s} = O(10^{-4})$. Hence, like δ_D , they are of interest in the context of physics beyond the SM [11,12].

With the advent of B factories and HERA-B, one expects that a large number of CP asymmetries in partial decay rates of B hadrons and rare B decays will become accessible to experimental and theoretical studies. Of particular interest in this context are the flavour-changing neutral-current (FCNC) processes which at the quark level can be thought of as taking place through induced $b \rightarrow d$ and $b \rightarrow s$ transitions. In terms of actual laboratory measurements, these FCNC processes will lead to $\Delta B = 1$, $\Delta Q = 0$ decays such as $B \rightarrow (X_s, X_d)l^+l^-$ and $B \rightarrow (X_s, X_d)\gamma$, where $X_s(X_d)$ represents an inclusive hadronic state with an overall quantum number $S = \pm 1(0)$, as well as their exclusive decay counterparts, such as $B \rightarrow (K, K^*, \pi, \rho, \dots)l^+l^-$ and $B \rightarrow (K^*, \rho, \omega, \dots)\gamma$. Of these, the decays $B \rightarrow X_s\gamma$ and $B \rightarrow K^*\gamma$ have already been measured [2]. The $\Delta B = 2$, $\Delta Q = 0$ transitions lead to $B_d^0-\overline{B}_d^0$ and $B_s^0-\overline{B}_s^0$ mixings, briefly discussed above. Likewise, non-trivial bounds have been put on the CP-violating phase $\sin 2\beta$ from the time-dependent rate asymmetry in the decays $B^0/\overline{B}^0 \rightarrow J/\psi K_s$ [13]. In K decays, the long sought after effect involving direct CP violation has been finally established through the measurement of the ratio ϵ'/ϵ [14,15]. This and the measurement of the CP-violating quantity $|\epsilon|$ in $K_L \rightarrow \pi\pi$ decays [2] represent the $s \rightarrow d$ FCNC transitions. Likewise, there exists great interest in the studies of FCNC rare

K decays such as $K^+ \rightarrow \pi^+ \nu \bar{\nu}$ and $K_L \rightarrow \pi^0 \nu \bar{\nu}$ [16], of which a single event has been measured in the former decay mode [17].

The FCNC processes and CP asymmetries in K and B decays provide stringent tests of the SM. The short-distance contributions to these transitions are dominated by the top quark, and hence these decays and asymmetries provide information on the weak mixing angles and phases in the matrix elements V_{td} , V_{ts} and V_{tb} of the CKM matrix. Some information on the last of these matrix elements is also available from the direct production and decay of the top quarks at the Fermilab Tevatron [18]. The measurement of V_{tb} will become quite precise at the LHC and linear colliders. Moreover, with advances in determining the (quark) flavour of a hadronic jet, one also anticipates being able to measure the matrix element V_{ts} (and possibly also V_{td}).

We shall concentrate here on the analysis of the data at hand and in forthcoming experiments which will enable us to test precisely the unitarity of the CKM matrix. These tests will be carried out in the context of the Unitarity Triangles (UT). The sides of UTs will be measured in K and B decays and the angles of these UTs will be measured by CP asymmetries. Consistency of a theory, such as the SM, requires that the two sets of independent measurements yield the same values of the CKM parameters, or, equivalently the CP-violating phases α , β and γ . We are tacitly assuming that there is only one CP-violating phase in weak interactions. This is the case in the SM but also in a number of variants of Supersymmetric Models, which, however, do have additional contributions to the FCNC amplitudes. In fact, it is the possible effect of these additional contributions which will be tested. In this case, quantitative predictions can be made which, in principle, allow experiments to discriminate among these theories [19]. As we shall see, the case for distinguishing the SM and the MSSM rests on the experimental and theoretical precision that can be achieved in various input quantities. Of course, there are many other theoretical scenarios in which deviations from the pattern of flavour violation in the SM are not minimal. For example, in the context of supersymmetric models, one may have non-diagonal quark-squark-gluino couplings, which also contain additional phases. These can contribute significantly to the magnitude and phase of $b \rightarrow d$, $b \rightarrow s$ and $s \rightarrow d$ transitions, which would then violate the SM flavour-violation pattern rather drastically. In this case it is easier to proclaim large deviations from the SM but harder to make quantitative predictions.

This paper is organized as follows. In Section 2, we discuss the profile of the unitarity triangle within the SM. We describe the input data used in the fits and present the allowed region in ρ - η space, as well as the presently-allowed ranges for the CP angles α , β and γ . We also discuss the fits in the superweak scenario, which differs from the SM fits in that we no longer use the constraint from the CP-violating quantity $|\epsilon|$. The superweak fits are not favoured by the

data and we quantify this in terms of the 95% C.L. exclusion contours. We turn to supersymmetric models in Section 3. We review several variants of the MSSM, in which the new phases are essentially zero. Restricting ourselves to flavour violation in charged-current transitions, we include the effects of charged Higgses H^\pm , a light scalar top quark (assumed here right-handed as suggested by the precision electroweak fits) and chargino χ^\pm . In this scenario, which covers an important part of the SUSY parameter space, the SUSY contributions to $K^0-\overline{K}^0$, $B_d^0-\overline{B}_d^0$ and $B_s^0-\overline{B}_s^0$ mixing are of the same form and can be characterized by a single parameter f . Including the NLO corrections in such models, we compare the profile of the unitarity triangle in SUSY models, for various values of f , with that of the SM. We conclude in Section 4.

2 Unitarity Triangle: SM Profile

Within the standard model (SM), CP violation is due to the presence of a nonzero complex phase in the Cabibbo-Kobayashi-Maskawa (CKM) quark mixing matrix V [3]. A particularly useful parametrization of the CKM matrix, due to Wolfenstein [20], follows from the observation that the elements of this matrix exhibit a hierarchy in terms of λ , the Cabibbo angle. In this parametrization the CKM matrix can be written approximately as

$$V \simeq \begin{pmatrix} 1 - \frac{1}{2}\lambda^2 & \lambda & A\lambda^3(\rho - i\eta) \\ -\lambda(1 + iA^2\lambda^4\eta) & 1 - \frac{1}{2}\lambda^2 & A\lambda^2 \\ A\lambda^3(1 - \rho - i\eta) & -A\lambda^2 & 1 \end{pmatrix}. \quad (5)$$

The allowed region in ρ - η space can be elegantly displayed using the so-called unitarity triangle (UT). The unitarity of the CKM matrix leads to the following relation:

$$V_{ud}V_{ub}^* + V_{cd}V_{cb}^* + V_{td}V_{tb}^* = 0. \quad (6)$$

Using the form of the CKM matrix in Eq. (5), this can be recast as

$$\frac{V_{ub}^*}{\lambda V_{cb}} + \frac{V_{td}}{\lambda V_{cb}} = 1, \quad (7)$$

which is a triangle relation in the complex plane (i.e. ρ - η space), illustrated in Fig. 1. Thus, allowed values of ρ and η translate into allowed shapes of the unitarity triangle.

Constraints on ρ and η come from a variety of sources. Of the quantities shown in Fig. 1, $|V_{cb}|$ and $|V_{ub}|$ can be extracted from semileptonic B decays,

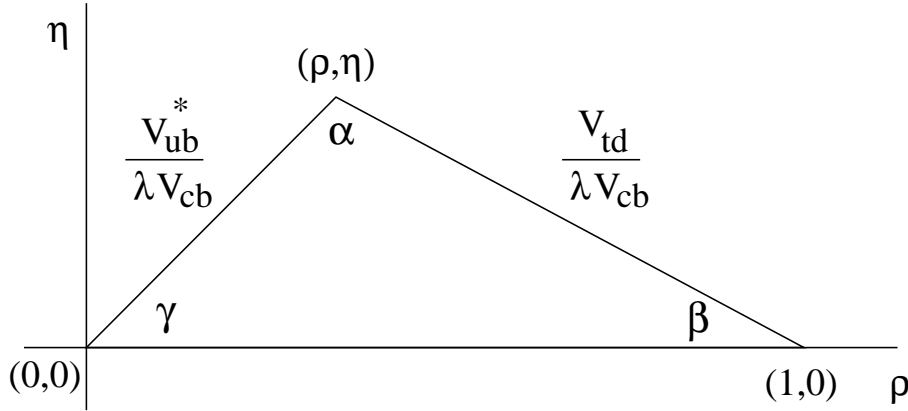


Fig. 1. *The unitarity triangle. The angles α , β and γ can be measured via CP violation in the B system.*

while $|V_{td}|$ is probed in $B_d^0-\overline{B}_d^0$ mixing. The interior CP-violating angles α , β and γ can be measured through CP asymmetries in B decays [21]. Additional constraints come from CP violation in the kaon system ($|\epsilon|$), as well as $B_s^0-\overline{B}_s^0$ mixing. As the constraints that are expected to come from the rare B and K decays mentioned earlier are not of interest for the CKM phenomenology at present, we shall not include them in our fits.

2.1 Input Data

The CKM matrix as parametrized in Eq. (5) depends on four parameters: λ , A , ρ and η . We summarize below the experimental and theoretical data which constrain these CKM parameters.

- $|V_{us}|$, $|V_{cb}|$ and $|V_{ub}/V_{cb}|$:

We recall that $|V_{us}|$ has been extracted with good accuracy from $K \rightarrow \pi e \nu$ and hyperon decays [2] to be $|V_{us}| = \lambda = 0.2196 \pm 0.0023$. The determination of $|V_{cb}|$ is based on the combined analysis of the inclusive and exclusive B decays: $|V_{cb}| = 0.0395 \pm 0.0017$ [2], yielding $A = 0.819 \pm 0.035$. The knowledge of the CKM matrix element ratio $|V_{ub}/V_{cb}|$ is based on the analysis of the end-point lepton energy spectrum in semileptonic decays $B \rightarrow X_u \ell \nu_\ell$ and the measurement of the exclusive semileptonic decays $B \rightarrow (\pi, \rho) \ell \nu_\ell$. Present measurements in both the inclusive and exclusive modes are compatible with $|V_{ub}/V_{cb}| = 0.093 \pm 0.014$ [10]. This gives $\sqrt{\rho^2 + \eta^2} = 0.423 \pm 0.064$.

- $|\epsilon|$, \hat{B}_K :

The experimental value of $|\epsilon|$ is [2]:

$$|\epsilon| = (2.280 \pm 0.013) \times 10^{-3} . \quad (8)$$

In the standard model, $|\epsilon|$ is essentially proportional to the imaginary part of the box diagram for $K^0-\overline{K}^0$ mixing and is given by [22]

$$|\epsilon| = \frac{G_F^2 f_K^2 M_K M_W^2}{6\sqrt{2}\pi^2 \Delta M_K} \hat{B}_K \left(A^2 \lambda^6 \eta \right) (y_c \{ \hat{\eta}_{ct} f_3(y_c, y_t) - \hat{\eta}_{cc} \} + \hat{\eta}_{tt} y_t f_2(y_t) A^2 \lambda^4 (1 - \rho)), \quad (9)$$

where $y_i \equiv m_i^2/M_W^2$, and the functions f_2 and f_3 are the Inami-Lim functions [23]. Here, the $\hat{\eta}_i$ are QCD correction factors, calculated at next-to-leading order: $(\hat{\eta}_{cc})$ [24], $(\hat{\eta}_{tt})$ [25] and $(\hat{\eta}_{ct})$ [26]. The theoretical uncertainty in the expression for $|\epsilon|$ is in the renormalization-scale independent parameter \hat{B}_K , which represents our ignorance of the matrix element $\langle K^0 | (\overline{d}\gamma^\mu(1 - \gamma_5)s)^2 | \overline{K}^0 \rangle$. Recent calculations of \hat{B}_K using lattice QCD methods are summarized at the 1998 summer conferences by Draper [27] and Sharpe [28], yielding

$$\hat{B}_K = 0.94 \pm 0.15. \quad (10)$$

- $\Delta M_d, f_{B_d}^2 \hat{B}_{B_d}$:

The present world average for ΔM_d is [9]

$$\Delta M_d = 0.471 \pm 0.016 \text{ (ps)}^{-1} . \quad (11)$$

The mass difference ΔM_d is calculated from the $B_d^0-\overline{B}_d^0$ box diagram, dominated by t -quark exchange:

$$\Delta M_d = \frac{G_F^2}{6\pi^2} M_W^2 M_B \left(f_{B_d}^2 \hat{B}_{B_d} \right) \hat{\eta}_B y_t f_2(y_t) |V_{td}^* V_{tb}|^2 , \quad (12)$$

where, using Eq. (5), $|V_{td}^* V_{tb}|^2 = A^2 \lambda^6 [(1 - \rho)^2 + \eta^2]$. Here, $\hat{\eta}_B$ is the QCD correction, which has the value $\hat{\eta}_B = 0.55$, calculated in the \overline{MS} scheme [25].

For the B system, the hadronic uncertainty is given by $f_{B_d}^2 \hat{B}_{B_d}$. Present estimates of this quantity using lattice QCD yield $f_{B_d} \sqrt{\hat{B}_{B_d}} = (190 \pm 23) \text{ MeV}$ in the quenched approximation [27,28]. The effect of unquenching is not yet understood completely. Taking the MILC collaboration estimates of unquenching would increase the central value of $f_{B_d} \sqrt{\hat{B}_{B_d}}$ by 21 MeV [29]. In the fits discussed here [19], the following range has been used:

$$f_{B_d} \sqrt{\hat{B}_{B_d}} = 215 \pm 40 \text{ MeV} . \quad (13)$$

Parameter	Value
λ	0.2196
$ V_{cb} $	0.0395 ± 0.0017
$ V_{ub}/V_{cb} $	0.093 ± 0.014
$ \epsilon $	$(2.280 \pm 0.013) \times 10^{-3}$
ΔM_d	$(0.471 \pm 0.016) (ps)^{-1}$
ΔM_s	$> 12.4 (ps)^{-1}$
$\overline{m}_t(m_t(pole))$	$(165 \pm 5) \text{ GeV}$
$\overline{m}_c(m_c(pole))$	$1.25 \pm 0.05 \text{ GeV}$
$\hat{\eta}_B$	0.55
$\hat{\eta}_{cc}$	1.38 ± 0.53
$\hat{\eta}_{ct}$	0.47 ± 0.04
$\hat{\eta}_{tt}$	0.57
\hat{B}_K	0.94 ± 0.15
$f_{B_d} \sqrt{\hat{B}_{B_d}}$	$215 \pm 40 \text{ MeV}$
ξ_s	1.14 ± 0.06

Table 1

Data and theoretical input used in the CKM fits.

- $\Delta M_s, f_{B_s}^2 \hat{B}_{B_s}$:

The $B_s^0 - \overline{B}_s^0$ box diagram is again dominated by t -quark exchange, and the mass difference between the mass eigenstates ΔM_s is given by a formula analogous to that of Eq. (12):

$$\Delta M_s = \frac{G_F^2}{6\pi^2} M_W^2 M_{B_s} \left(f_{B_s}^2 \hat{B}_{B_s} \right) \hat{\eta}_{B_s} y_t f_2(y_t) |V_{ts}^* V_{tb}|^2. \quad (14)$$

Using the fact that $|V_{cb}| = |V_{ts}|$ (Eq. (5)), it is clear that one of the sides of the unitarity triangle, $|V_{td}/\lambda V_{cb}|$, can be obtained from the ratio of ΔM_d and ΔM_s ,

$$\frac{\Delta M_s}{\Delta M_d} = \frac{\hat{\eta}_{B_s} M_{B_s} \left(f_{B_s}^2 \hat{B}_{B_s} \right)}{\hat{\eta}_{B_d} M_{B_d} \left(f_{B_d}^2 \hat{B}_{B_d} \right)} \left| \frac{V_{ts}}{V_{td}} \right|^2. \quad (15)$$

The only real uncertainty in this quantity is the ratio of hadronic matrix elements $f_{B_s}^2 \hat{B}_{B_s} / f_{B_d}^2 \hat{B}_{B_d}$. The present estimate of this quantity is [27,28]

$$\xi_s = 1.14 \pm 0.06. \quad (16)$$

The present lower bound on ΔM_s is: $\Delta M_s > 12.4 (ps)^{-1}$ (at 95% C.L.) [10].

There are two other measurements which should be mentioned here. First, the KTEV collaboration [14] has recently reported a measurement of direct CP

violation in the K sector through the ratio ϵ'/ϵ , with

$$\text{Re}(\epsilon'/\epsilon) = (28.0 \pm 3.0(\text{stat}) \pm 2.6(\text{syst}) \pm 1.0(\text{MC stat})) \times 10^{-4}, \quad (17)$$

in agreement with the earlier measurement by the CERN experiment NA31 [15], which reported a value of $(23 \pm 6.5) \times 10^{-4}$ for the same quantity. The present world average is $\text{Re}(\epsilon'/\epsilon) = (21.8 \pm 3.0) \times 10^{-4}$. This combined result excludes the superweak model [30] by more than 7σ .

A great deal of theoretical effort has gone into calculating this quantity at next-to-leading order accuracy in the SM [31–33]. The result of this calculation can be summarized in the following form due to Buras and Silvestrini [34]:

$$\text{Re}(\epsilon'/\epsilon) = \text{Im}\lambda_t \left[-1.35 + R_s \left(1.1|r_Z^{(8)}|B_6^{(1/2)} + (1.0 - 0.67|r_Z^{(8)}|)B_8^{(3/2)} \right) \right]. \quad (18)$$

Here $\text{Im}\lambda_t = \text{Im}V_{td}V_{ts}^* = A^2\lambda^5\eta$, and $r_Z^{(8)}$ represents the short-distance contribution, which at the NLO precision is estimated to lie in the range $6.5 \leq |r_Z^{(8)}| \leq 8.5$ [31,32]. The quantities $B_6^{(1/2)} = B_6^{(1/2)}(m_c)$ and $B_8^{(3/2)} = B_8^{(3/2)}(m_c)$ are the matrix elements of the $\Delta I = 1/2$ and $\Delta I = 3/2$ operators O_6 and O_8 , respectively, calculated at the scale $\mu = m_c$. Lattice-QCD [35] and the $1/N_c$ expansion [36] yield:

$$0.8 \leq B_6^{(1/2)} \leq 1.3, \quad 0.6 \leq B_8^{(3/2)} \leq 1.0. \quad (19)$$

Finally, the quantity R_s in Eq. (18) is defined as:

$$R_s \equiv \left(\frac{150 \text{ MeV}}{m_s(m_c) + m_d(m_c)} \right)^2, \quad (20)$$

essentially reflecting the s -quark mass dependence. The present uncertainty on the CKM matrix element is $\pm 23\%$, which is already substantial. However, the theoretical uncertainties related to the other quantities discussed above are considerably larger. For example, the ranges $\epsilon'/\epsilon = (5.3 \pm 3.8) \times 10^{-4}$ and $\epsilon'/\epsilon = (8.5 \pm 5.9) \times 10^{-4}$, assuming $m_s(m_c) = 150 \pm 20 \text{ MeV}$ and $m_s(m_c) = 125 \pm 20 \text{ MeV}$, respectively, have been quoted as the best representation of the status of ϵ'/ϵ in the SM [16]. These estimates are somewhat on the lower side compared to the data but not inconsistent.

Thus, whereas ϵ'/ϵ represents a landmark measurement, establishing for the first time direct CP-violation in decay amplitudes, and hence removing the superweak model of Wolfenstein and its various incarnations from further consideration, its impact on CKM phenomenology, particularly in constraining

the CKM parameters, is marginal. For this reason, the measurement of ϵ'/ϵ is not included in the CKM fits summarized here.

Second, the CDF collaboration has recently made a measurement of $\sin 2\beta$ [13]. In the Wolfenstein parametrization, $-\beta$ is the phase of the CKM matrix element V_{td} . From Eq. (5) one can readily find that

$$\sin(2\beta) = \frac{2\eta(1-\rho)}{(1-\rho)^2 + \eta^2} . \quad (21)$$

Thus, a measurement of $\sin 2\beta$ would put a strong constraint on the parameters ρ and η . However, the CDF measurement gives [13]

$$\sin 2\beta = 0.79^{+0.41}_{-0.44} , \quad (22)$$

or $\sin 2\beta > 0$ at 93% C.L. This constraint is quite weak – the indirect measurements already constrain $0.52 \leq \sin 2\beta \leq 0.94$ at the 95% C.L. in the SM [19]. (The CKM fits reported recently in the literature [10,38,39] yield similar ranges.) In light of this, this measurement is not included in the fits. The data used in the CKM fits are summarized in Table 1.

2.2 SM Fits

In the fit presented here [19], ten parameters are allowed to vary: ρ , η , A , m_t , m_c , η_{cc} , η_{ct} , $f_{B_d}\sqrt{\hat{B}_{B_d}}$, \hat{B}_K , and ξ_s . The ΔM_s constraint is included using the amplitude method [37]. The rest of the parameters are fixed to their central values. The allowed (95% C.L.) ρ - η region is shown in Fig. 2. The best-fit values of the CKM parameters are:

$$\lambda = 0.2196 \text{ (fixed)}, \quad A = 0.817, \quad \rho = 0.196, \quad \eta = 0.37 . \quad (23)$$

The “best-fit” values of the CKM matrix elements are as follows (Note that we have rounded all elements except V_{ub} and V_{td} to the nearest 0.005):

$$V \simeq \begin{pmatrix} 0.975 & 0.220 & 0.002 - 0.003i \\ -0.220 & 0.975 & 0.040 \\ 0.007 - 0.003i & -0.040 & 1 \end{pmatrix} . \quad (24)$$

Now, turning to the ratios of CKM matrix elements, which one comes across in the CKM phenomenology, the “best-fit” values are:

$$\left| \frac{V_{td}}{V_{ts}} \right| = 0.19, \quad \left| \frac{V_{td}}{V_{ub}} \right| = 2.12, \quad \left| \frac{V_{ub}}{V_{cb}} \right| = 0.091 . \quad (25)$$

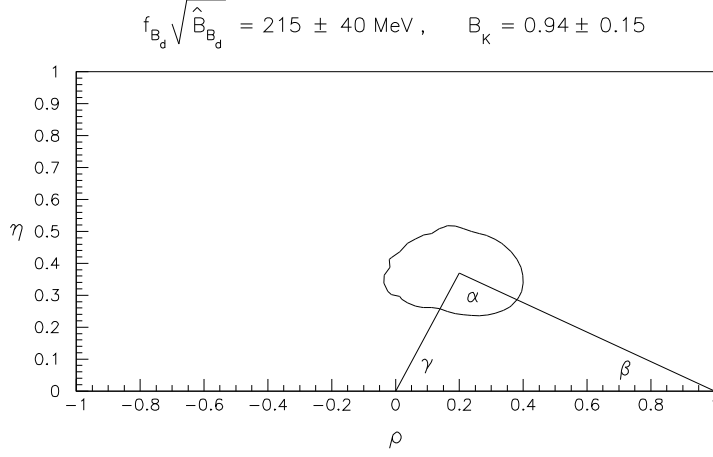


Fig. 2. Allowed region in ρ - η space in the SM, from a fit to the ten parameters discussed in the text and given in Table 1. The limit on ΔM_s is included using the amplitude method [37]. The theoretical errors on $f_{B_d} \sqrt{\hat{B}_{B_d}}$, \hat{B}_K and ξ_s are treated as Gaussian. The solid line represents the region with $\chi^2 = \chi_{min}^2 + 6$ corresponding to the 95% C.L. region. The triangle shows the best fit. (From Ref. [19].)

The 95% C.L. ranges are:

$$0.15 \leq \left| \frac{V_{td}}{V_{ts}} \right| \leq 0.24 , \quad 1.30 \leq \left| \frac{V_{td}}{V_{ub}} \right| \leq 3.64 , \quad 0.06 \leq \left| \frac{V_{ub}}{V_{cb}} \right| \leq 0.125 . \quad (26)$$

With the above fits, the “best-fit” value of ΔM_s is $\Delta M_s = 16.6 \text{ (ps)}^{-1}$. The corresponding 95% C.L. allowed range is:

$$12.4 \text{ (ps)}^{-1} \leq \Delta M_s \leq 27.9 \text{ (ps)}^{-1} . \quad (27)$$

The CP angles α , β and γ can be measured in CP-violating rate asymmetries in B decays. These angles can be expressed in terms of ρ and η . Thus, different shapes of the unitarity triangle are equivalent to different values of the CP angles. Referring to Fig. 2, we note that the preferred (central) values of these angles are $(\alpha, \beta, \gamma) = (93^\circ, 25^\circ, 62^\circ)$. The allowed ranges at 95% C.L. are

$$65^\circ \leq \alpha \leq 123^\circ , \quad 16^\circ \leq \beta \leq 35^\circ , \quad 36^\circ \leq \gamma \leq 97^\circ . \quad (28)$$

These ranges are similar to the ones obtained in [38,39], but not identical as the input parameters differ.

Of course, the values of α , β and γ are correlated, i.e. they are not all allowed simultaneously. We illustrate these correlations in Figs. 3 and 4. Fig. 3 shows the allowed region in $\sin 2\alpha$ – $\sin 2\beta$ space allowed by the data. And Fig. 4 shows the allowed (correlated) values of the CP angles α and γ . This correlation is roughly linear, due to the relatively small allowed range of β (Eq. (28)).

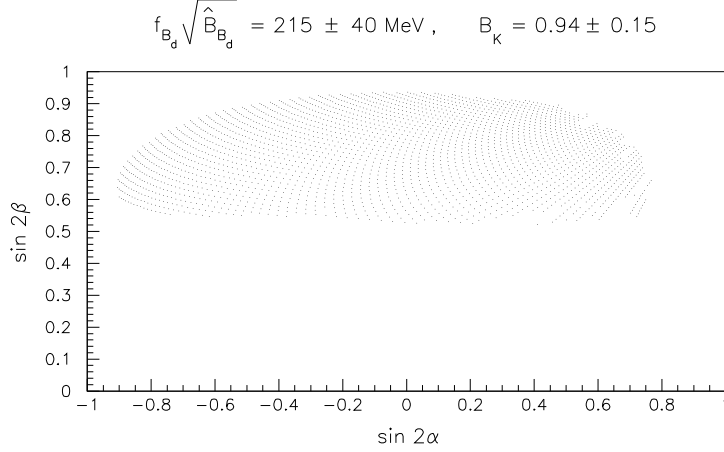


Fig. 3. Allowed 95% C.L. region of the CP-violating quantities $\sin 2\alpha$ and $\sin 2\beta$ in the SM, from a fit to the data given in Table 1. (From Ref. [19].)

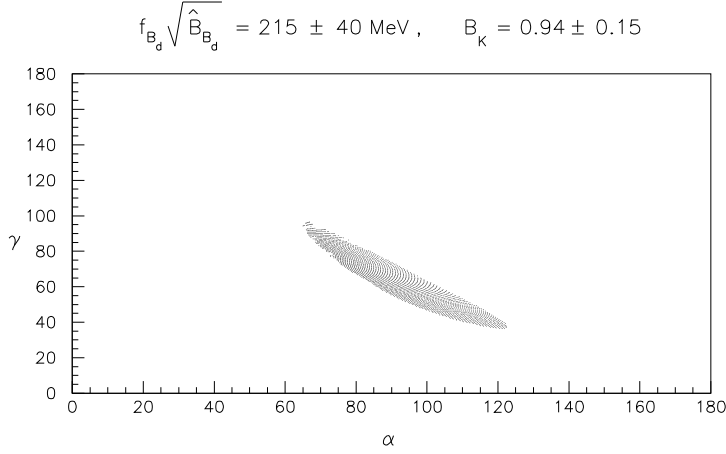


Fig. 4. Allowed 95% C.L. region of the CP-violating quantities α and γ in the SM, from a fit to the data given in Table 1. (From Ref. [19].)

2.3 CKM Fits in Superweak Theories

As we mentioned earlier, superweak theories of CP violation are now ruled out by the measurements of the ratio ϵ'/ϵ [14,15]. We show in this section that a non-trivial constraint on the CKM phase η also results from the present data leaving out the information on $|\epsilon|$ (we have not included the measurement of ϵ'/ϵ in the analysis either, as discussed in the context of our SM-based fits presented earlier). The input parameters for this fit are given in Table 1, except that now we leave out $|\epsilon|$ and \hat{B}_K from the analysis. Thus, we have one data input less compared to the SM-fit and only nine parameters to fit (compared to ten in the SM-case).

The most sensitive theoretical parameter in the fits is now $f_{B_d} \sqrt{\hat{B}_{B_d}}$. To show

the dependence of the allowed CKM-parameter space on this quantity, we fix its value in performing the fits and vary it in the range $170 \text{ MeV} \leq f_{B_d}\sqrt{\hat{B}_{B_d}} \leq 280 \text{ MeV}$. The results for the allowed 95% C.L. contour are shown in Fig. 5 for the six values $f_{B_d}\sqrt{\hat{B}_{B_d}} = 190, 210, 220, 240, 260$ and 280 MeV . The resulting unitarity triangle for the choice $f_{B_d}\sqrt{\hat{B}_{B_d}} = 170 \text{ MeV}$ is very similar to one shown for $f_{B_d}\sqrt{\hat{B}_{B_d}} = 190 \text{ MeV}$ and hence we do not display it. The triangle drawn in each case is the best-fit solution. From these figures we see that the case $\eta = 0$ (superweak model) is ruled out for all values of $f_{B_d}\sqrt{\hat{B}_{B_d}}$ in the Lattice-QCD range $f_{B_d}\sqrt{\hat{B}_{B_d}} = 215 \pm 40 \text{ MeV}$. Only for very high values of $f_{B_d}\sqrt{\hat{B}_{B_d}}$, illustrated here by the case $f_{B_d}\sqrt{\hat{B}_{B_d}} = 280 \text{ MeV}$, is the superweak theory still compatible with data. Restricting to the range $190 \text{ MeV} \leq f_{B_d}\sqrt{\hat{B}_{B_d}} \leq 240 \text{ MeV}$, given by the upper four plots in Fig. 5, we see that at 95% C.L. the CKM-phase η is determined to lie in the range $0.20 \leq \eta \leq 0.55$. This can also be seen in Fig. 6 (uppermost of the three curves), where we show the resulting 95% C.L. allowed contour using $f_{B_d}\sqrt{\hat{B}_{B_d}} = 215 \pm 25 \text{ MeV}$, but assuming that the errors are Gaussian distributed. A comparison of the allowed (ρ - η)-contours in Figs. 5 and 6 also shows that the specific distribution assumed for the theoretical error is not crucial. Thus, with the input $f_{B_d}\sqrt{\hat{B}_{B_d}} = 215 \pm 25 \text{ MeV}$, present data predict a value of η well within a factor 3. However, the assumption on the error of $f_{B_d}\sqrt{\hat{B}_{B_d}}$ does play a significant role in determining the allowed range of η . For example, using $f_{B_d}\sqrt{\hat{B}_{B_d}} = 215 \pm 40 \text{ MeV}$ as input, the 95% C.L. allowed contour comes close to the ρ -axis, making the superweak value $\eta = 0$ just barely incompatible with data. This is shown in Fig. 6 (second of the three curves shown here). The superweak theory becomes compatible with the available data if the theoretical error on $f_{B_d}\sqrt{\hat{B}_{B_d}}$ is further increased to $\pm 60 \text{ MeV}$. The resulting contour for $f_{B_d}\sqrt{\hat{B}_{B_d}} = 215 \pm 60 \text{ MeV}$ is displayed in Fig. 6 (lowest of the three curves).

We conclude that with the present theoretical knowledge $f_{B_d}\sqrt{\hat{B}_{B_d}} = 215 \pm 40 \text{ MeV}$, the superweak case is ruled out at 95% C.L. from the CKM fits, though the value of η is not determined precisely.

3 Unitarity Triangle: A SUSY Profile

In this section we examine the profile of the unitarity triangle in supersymmetric (SUSY) theories. The most general models contain a number of unconstrained phases and so are not sufficiently predictive to perform such an analysis. However, there is a class of SUSY models in which these phases are

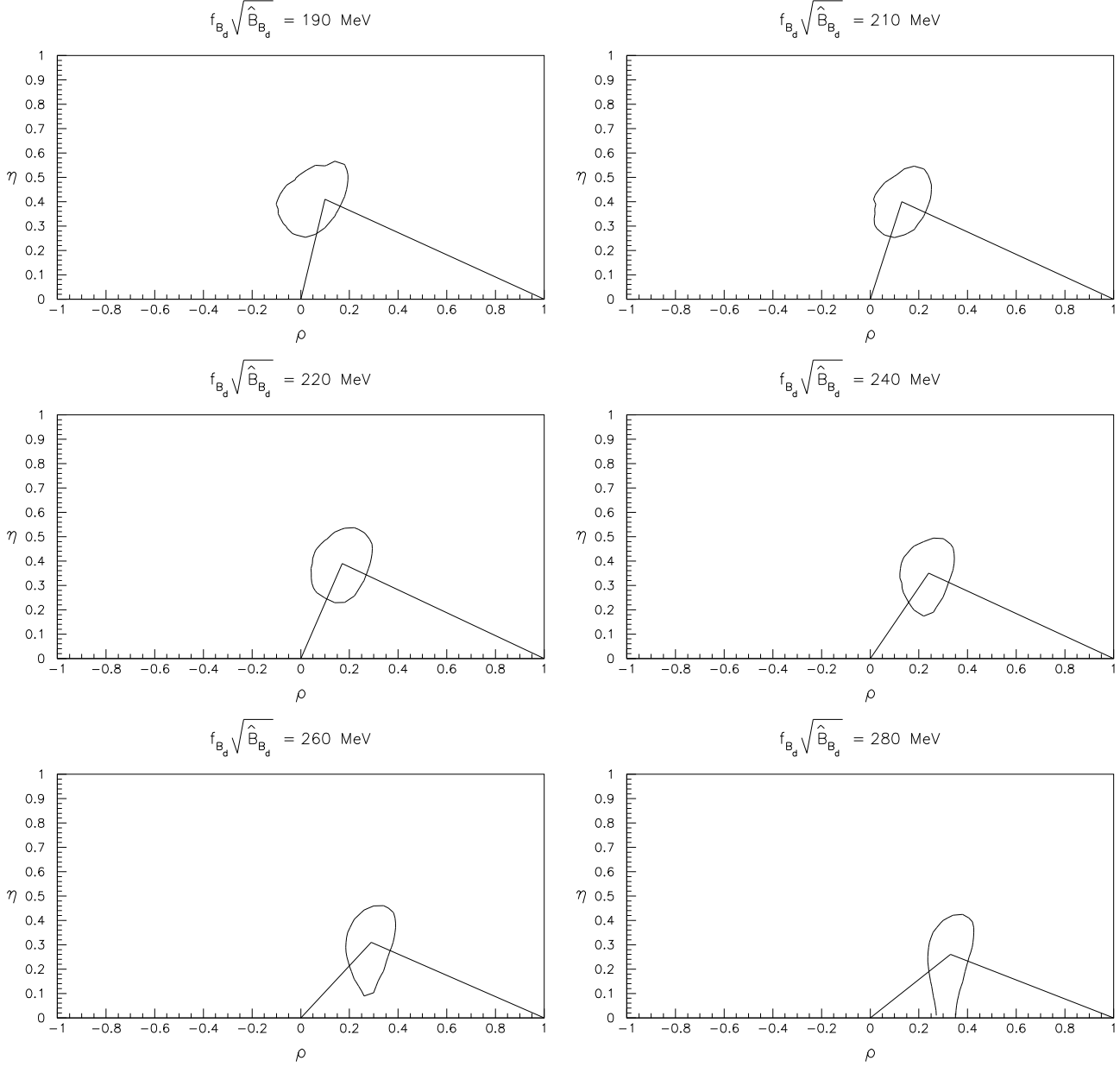


Fig. 5. Allowed regions in ρ - η space in the Superweak theories obtained by leaving out the constraint from $|\epsilon|$, and performing a fit to the remaining parameters given in Table 1. The limit on ΔM_s is included using the amplitude method [37]. The input values for $f_{B_d} \sqrt{\hat{B}_{B_d}}$ are shown on top of the individual figures. The solid lines represent the region with $\chi^2 = \chi^2_{\min} + 6$ corresponding to the 95% C.L. region. The triangles show the best fits.

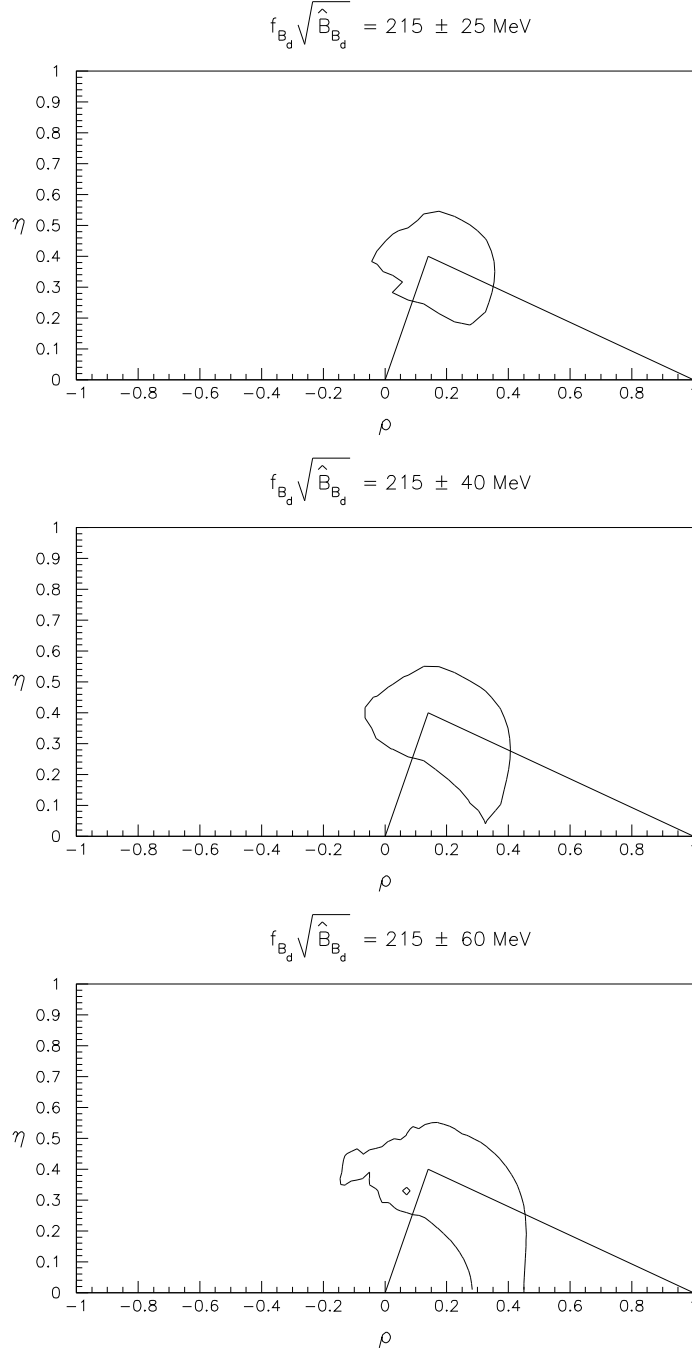


Fig. 6. Allowed regions in ρ - η space in the Superweak theories obtained by leaving out the constraint from $|\epsilon|$, and performing a fit to the remaining parameters given in Table 1, assuming that theoretical errors are Gaussian-distributed. The limit on ΔM_s is included using the amplitude method [37]. The input values for $f_{B_d} \sqrt{\hat{B}_{B_d}}$ used in the fits are shown on top of the individual figures. The solid lines represent the region with $\chi^2 = \chi_{min}^2 + 6$ corresponding to the 95% C.L. region. The triangles show the best fits.

constrained to be approximately zero, which greatly increases the predictivity. In the following subsections, we discuss aspects of more general SUSY theories, as well as the details of that class of theories whose effects on the unitarity triangle can be directly analyzed.

3.1 Flavour Violation in SUSY Models - Overview

We begin with a brief review of flavour violation in the minimal supersymmetric standard model (MSSM).

The low energy effective theory in the MSSM can be specified in terms of the chiral superfields for the three generations of quarks (Q_i , U_i^c , and D_i^c) and leptons (L_i and E_i^c), chiral superfields for two Higgs doublets (H_1 and H_2), and vector superfields for the gauge group $SU(3)_C \times SU(2)_I \times U(1)_Y$ [40]. The superpotential is given by

$$W_{MSSM} = f_D^{ij} Q_i D_j H_1 + f_U^{ij} Q_i U_j H_2 + f_L^{ij} E_i L_j H_1 + \mu H_1 H_2. \quad (29)$$

The indices $i, j = 1, 2, 3$ are generation indices and f_D^{ij} , f_U^{ij} , f_L^{ij} are Yukawa coupling matrices in the generation space. A general form of the soft SUSY-breaking term is given by

$$\begin{aligned} -L_{\text{soft}} = & (m_Q^2)_j^i \tilde{q}_i \tilde{q}^{\dagger j} + (m_D^2)_j^i \tilde{d}_i \tilde{d}^{\dagger j} + (m_U^2)_j^i \tilde{u}_i \tilde{u}^{\dagger j} + (m_E^2)_j^i \tilde{e}_i \tilde{e}^{\dagger j} \\ & + (m_L^2)_j^i \tilde{\ell}_i \tilde{\ell}^{\dagger j} + \Delta_1^2 h_1^\dagger h_1 + \Delta_2^2 h_2^\dagger h_2 - (B\mu h_1 h_2 + h.c.) \\ & + (A_D^{ij} \tilde{q}_i \tilde{d}_j h_1 + A_U^{ij} \tilde{q}_i \tilde{u}_j h_2 + A_L^{ij} \tilde{e}_i \tilde{\ell}_j h_1 + h.c.) \\ & + \left(\frac{M_1}{2} \tilde{B} \tilde{B} + \frac{M_2}{2} \tilde{W} \tilde{W} + \frac{M_3}{2} \tilde{G} \tilde{G} + h.c. \right), \end{aligned} \quad (30)$$

where \tilde{q}_i , \tilde{u}_i , \tilde{d}_i , $\tilde{\ell}_i$, \tilde{e}_i , h_1 and h_2 are scalar components of the superfields Q_i , U_i , D_i , L_i , E_i , H_1 and H_2 , respectively, and \tilde{B} , \tilde{W} and \tilde{G} are the $U(1)$, $SU(2)$ and $SU(3)$ gauge fermions, respectively. The SUSY-breaking parameters $(m_F)_j^i$, with $m_F = m_D, m_U, m_L, m_E$ and the trilinear scalar couplings A_D^{ij} , A_U^{ij} and A_L^{ij} are 3×3 matrices in the flavour space. It is obvious that supersymmetric theories have an incredibly complicated flavour structure, resulting in a large number of *a priori* unknown mixing angles, which cannot be determined theoretically. Present measurements and limits on the FCNC processes do provide some constraints on these mixing angles [41]. We shall not follow this route here.

Alternatively, one could put restrictions on the soft SUSY-breaking (SSB) terms. The ones most discussed in the literature are those which find their rationale in supergravity (SUGRA) models, in which it is assumed that the

SSB terms have universal structures at the Planck scale, following from the assumption that the hidden sector of $N = 1$ SUGRA theory is flavour-blind. This results in the universal scalar mass, m_0 , with $(m_Q^2)_j^i = (m_E^2)_j^i = \dots = m_0^2 \delta_j^i$; $\Delta_1^2 = \Delta_2^2 = \Delta_0^2$, universal A -terms, $A_D^{ij} = f_D^{ij} A m_0$, etc., and universal gaugino masses M_g , defined as $M_1 = M_2 = M_3 = M_g$. These universal structures are required in order to suppress FCNC processes. The scenario with the additional constraint $m_0 = \Delta_0$ is called the minimal SUGRA model. In other theoretical scenarios, it is not necessary to invoke universal SSB terms. In order to make testable predictions it is sufficient to restrict all flavour violations in the charged-current sector, which are determined by the known CKM angles [42]. We shall be mostly dealing here with this scenario, known as *minimal flavour violation*, as well as SUGRA-type scenarios.

Even in these restricted scenarios, one is confronted with the complex phases residing in the W_{MSSM} and L_{soft} part of the supersymmetric lagrangian. In general, MSSM models have three physical phases, apart from the QCD vacuum parameter $\bar{\theta}_{QCD}$ which we shall take to be zero. The three phases are: (i) the CKM phase represented here by the Wolfenstein parameter η , (ii) the phase $\theta_A = \arg(A)$, and (iii) the phase $\theta_\mu = \arg(\mu)$ [43]. The last two phases are peculiar to SUSY models and their effects must be taken into account in a general supersymmetric framework. In particular, the CP-violating asymmetries which result from the interference between mixing and decay amplitudes can produce non-standard effects. Concentrating here on the $\Delta B = 2$ amplitudes, two new phases θ_d and θ_s arise, which can be parametrized as follows [44]:

$$\theta_{d,s} = \frac{1}{2} \arg \left(\frac{\langle B_{d,s} | H_{eff}^{SUSY} | \bar{B}_{d,s} \rangle}{\langle B_{d,s} | H_{eff}^{SM} | \bar{B}_{d,s} \rangle} \right), \quad (31)$$

where H^{SUSY} is the effective Hamiltonian including both the SM degrees of freedom and the SUSY contributions. Thus, CP-violating asymmetries in B decays would involve not only the phases α , β and γ , defined previously, but additionally θ_d or θ_s . In other words, the SUSY contributions to the real parts of $M_{12}(B_d)$ and $M_{12}(B_s)$ are *no longer proportional* to the CKM matrix elements $V_{td}V_{tb}^*$ and $V_{ts}V_{tb}^*$, respectively. If θ_d or θ_s were unconstrained, one could not make firm predictions about the CP asymmetries in SUSY models. In this case, an analysis of the profile of the unitarity triangle in such models would be futile.

However, the experimental upper limits on the electric dipole moments (EDM) of the neutron and electron [2] do provide constraints on the phases θ_μ and θ_A [45]. In SUGRA models with *a priori* complex parameters A and μ , the phase θ_μ is strongly bounded with $\theta_\mu < 0.01\pi$ [46]. The phase θ_A can be of $O(1)$ in the small θ_μ region, as far as the EDMs are concerned. In both

the $\Delta S = 2$ and $\Delta B = 2$ transitions, and for low-to-moderate values of $\tan v$ ¹, it has been shown that θ_A does not change the phase of either the matrix element $M_{12}(K)$ [43] or of $M_{12}(B)$ [46]. Hence, in SUGRA models, $\arg M_{12}(B)|_{SUGRA} = \arg M_{12}(B)|_{SM} = \arg(\xi_t^2)$, where $\xi_t = V_{td}^* V_{tb}$. Likewise, the phase of the SUSY contribution in $M_{12}(K)$ is aligned with the phase of the $t\bar{t}$ -contribution in $M_{12}(K)$, given by $\arg(V_{td} V_{ts}^*)$. Thus, in these models, one can effectively set $\theta_d \simeq 0$ and $\theta_s \simeq 0$, so that the CP-violating asymmetries give information about the SM phases α , β and γ . Hence, an analysis of the UT and CP-violating phases α , β and γ can be carried out in a very similar fashion as in the SM, taking into account the additional contributions to $M_{12}(K)$ and $M_{12}(B)$.

For large- $\tan v$ solutions, one has to extend the basis of $H_{eff}(\Delta B = 2)$ so as to include new operators whose contribution is small in the low- $\tan v$ limit. The resulting effective Hamiltonian is given by

$$H_{eff}(\Delta B = 2) = \frac{G_F^2 M_W^2}{2\pi^2} \sum_{i=1}^3 C_i(\mu) O_i, \quad (32)$$

where $O_1 = \bar{d}_L^\alpha \gamma_\mu b_L^\alpha \bar{d}_L^\beta \gamma^\mu b_L^\beta$, $O_2 = \bar{d}_L^\alpha b_R^\alpha \bar{d}_L^\beta b_R^\beta$ and $O_3 = \bar{d}_L^\alpha b_R^\beta \bar{d}_L^\beta b_R^\alpha$ and C_i are the Wilson coefficients [47,48]. The coefficients $C_1(\mu)$ and $C_2(\mu)$ are real relative to the SM contribution. However, the chargino contributions to $C_3(\mu)$ are generally complex relative to the SM contribution and can generate a new phase shift in the $B^0-\bar{B}^0$ mixing amplitude [49,50]. This effect is in fact significant for large $\tan v$ [47], since $C_3(\mu)$ is proportional to $(m_b/m_W \cos \beta)^2$. How large this additional phase (θ_d and θ_s) can be depends on how the constraints from EDM are imposed. For example, Baek and Ko [50] find that in the MSSM without imposing the EDM constraint, one has $2|\theta_d| \leq 6^\circ$ for a light stop and large $\tan v$ but this phase becomes practically zero if the EDM constraints [51] are imposed.

In view of the foregoing, we shall restrict ourselves to a class of SUSY models in which the following features, related to flavour mixing, hold:

- The squark flavour mixing matrix which diagonalizes the squark mass matrix is approximately the same as the corresponding quark mixing matrix V_{CKM} , apart from the left-right mixing of the top squarks.

¹ In supersymmetric jargon, the quantity $\tan \beta$ is used to define the ratio of the two vacuum expectation values (vevs) $\tan \beta \equiv v_u/v_d$, where $v_d(v_u)$ is the vev of the Higgs field which couples exclusively to down-type (up-type) quarks and leptons. (See, for example, the review by Haber in Ref. [2]). However, in discussing flavour physics, the symbol β is traditionally reserved for one of the angles of the unitarity triangle. To avoid confusion, we will call the ratio of the vevs $\tan v$.

- The phases θ_d and θ_s are negligible in the entire $\tan v$ plane, once the constraints from the EDMs of neutron and lepton are consistently imposed.
- The first- and second-generation squarks with the same quantum numbers remain highly degenerate in masses but the third-generation squarks, especially the top squark, can be significantly lighter due to the renormalization effect of the top Yukawa coupling constants.

These features lead to an enormous simplification in the flavour structure of the SUSY contributions to flavour-changing processes. In particular, SUSY contributions to the transitions $b \rightarrow s$, $b \rightarrow d$ and $s \rightarrow d$ are proportional to the CKM factors, $V_{tb}V_{ts}^*$, $V_{tb}V_{td}^*$ and $V_{ts}V_{td}^*$, respectively. Similarly, the SUSY contributions to the mass differences $M_{12}(B_s)$, $M_{12}(B_d)$ and $M_{12}(K)$ are proportional to the CKM factors $(V_{tb}V_{ts}^*)^2$, $(V_{tb}V_{td}^*)^2$ and $(V_{ts}V_{td}^*)^2$, respectively. These are precisely the same factors which govern the contribution of the top quark in these transitions in the standard model. Thus, the supersymmetric contributions can be implemented in a straightforward way by adding a (supersymmetric) piece in each of the above mentioned amplitudes to the corresponding top quark contribution in the SM.

3.2 NLO Corrections to ΔM_d , ΔM_s and ϵ in Minimal SUSY Flavour Violation

A number of SUSY models share the features mentioned in the previous subsection, and the supersymmetric contributions to the mass differences $M_{12}(B)$ and $M_{12}(K)$ have been analyzed in a number of papers [46,47,52–55], following the pioneering work of Ref. [56]. Following these papers, ΔM_d can be expressed as:

$$\Delta M_d = \frac{G_F^2}{6\pi^2} M_W^2 M_B \left(f_{B_d}^2 \hat{B}_{B_d} \right) \hat{\eta}_B \times [A_{SM}(B) + A_{H^\pm}(B) + A_{\chi^\pm}(B) + A_{\tilde{g}}(B)] , \quad (33)$$

where the function $A_{SM}(B)$ can be written by inspection from Eq. (12):

$$A_{SM}(B) = y_t f_2(y_t) |V_{td}^* V_{tb}|^2 . \quad (34)$$

The expressions for $A_{H^\pm}(B)$, $A_{\chi^\pm}(B)$ and $A_{\tilde{g}}(B)$ are obtained from the SUSY box diagrams. Here, H^\pm , χ_j^\pm , \tilde{t}_a and \tilde{d}_i represent, respectively, the charged Higgs, chargino, stop and down-type squarks. The contribution of the intermediate states involving neutralinos is small and usually neglected. The expressions for $A_{H^\pm}(B)$, $A_{\chi^\pm}(B)$ and $A_{\tilde{g}}(B)$ are given explicitly in the literature [47,52,56].

We shall not be using the measured value of the mass difference ΔM_K due to the uncertain contribution of the long-distance contribution. However, $|\epsilon|$ is a short-distance dominated quantity and in supersymmetric theories can be expressed as follows:

$$|\epsilon| = \frac{G_F^2 f_K^2 M_K M_W^2}{6\sqrt{2}\pi^2 \Delta M_K} \hat{B}_K [\text{Im } A_{SM}(K) + \text{Im } A_{H^\pm}(K) + \text{Im } A_{\chi^\pm}(K) + \text{Im } A_{\tilde{g}}(K)] , \quad (35)$$

where, again by inspection with the SM expression for $|\epsilon|$ given in Eq. (9), one has

$$\text{Im } A_{SM}(K) = A^2 \lambda^6 \eta(y_c \{ \hat{\eta}_{ct} f_3(y_c, y_t) - \hat{\eta}_{cc} \} + \hat{\eta}_{tt} y_t f_2(y_t) A^2 \lambda^4 (1 - \rho)). \quad (36)$$

The expressions for $\text{Im } A_{H^\pm}(K)$, $\text{Im } A_{\chi^\pm}(B)$ and $\text{Im } A_{\tilde{g}}(B)$ can be found in Refs. [47,52,56].

For the analysis reported here, we follow the scenario called *minimal flavour violation* in Ref. [42]. In this class of supersymmetric theories, apart from the SM degrees of freedom, only charged Higgses, charginos and a light stop (assumed to be right-handed) contribute, with all other supersymmetric particles integrated out. This scenario is effectively implemented in a class of SUGRA models (both minimal and non-minimal) and gauge-mediated models [57], in which the first two squark generations are heavy and the contribution from the intermediate gluino-squark states is small [46,52–55].

For these models, the next-to-leading-order (NLO) corrections for ΔM_d , ΔM_s and $|\epsilon|$ can be found in Ref. [58]. Moreover, the branching ratio $B(B \rightarrow X_s \gamma)$ has been calculated in Ref. [42]. We make use of this information and quantitatively examine the unitarity triangle, CP-violating asymmetries and their correlations for this class of supersymmetric theories. The phenomenological profiles of the unitarity triangle and CP phases for the SM and this class of supersymmetric models can thus be meaningfully compared. Given the high precision on the phases α , β and γ expected from experiments at B -factories and hadron colliders, a quantitative comparison of this kind could provide a means of discriminating between the SM and this class of MSSM's.

The NLO QCD-corrected effective Hamiltonian for $\Delta B = 2$ transitions in the minimal flavour violation SUSY framework can be expressed as follows [58]:

$$H_{eff} = \frac{G_F^2}{4\pi^2} (V_{td} V_{tb}^*)^2 \hat{\eta}_{2,S}(B) SO_{LL} , \quad (37)$$

where the NLO QCD correction factor $\hat{\eta}_{2,S}(B)$ is given by [58]:

$$\hat{\eta}_{2,S}(B) = \alpha_s(m_W) \gamma^{(0)} / (2\beta_{n_f}^{(0)}) \left[1 + \frac{\alpha_s(m_W)}{4\pi} \left(\frac{D}{S} + Z_{n_f} \right) \right], \quad (38)$$

in which n_f is the number of active quark flavours (here $n_f = 5$), the quantity Z_{n_f} is defined below, and $\gamma^{(0)}$ and $\beta_{n_f}^{(0)}$ are the lowest order perturbative QCD β -function and the anomalous dimension, respectively. The operator $O_{LL} = O_1$ is the one which is present in the SM, previously defined in the discussion following Eq. (32). The explicit expression for the function S can be obtained from Ref. [56] and for D it is given in Ref. [58], where it is derived in the NDR (naive dimensional regularization) scheme using \overline{MS} -renormalization.

The Hamiltonian given above for $B_d^0 - \overline{B}_d^0$ mixing leads to the mass difference

$$\Delta M_d = \frac{G_F^2}{6\pi^2} (V_{td} V_{tb}^*)^2 \hat{\eta}_{2,S}(B) S(f_{B_d}^2 \hat{B}_{B_d}). \quad (39)$$

The corresponding expression for ΔM_s is obtained by making the appropriate replacements. Since the QCD correction factors are identical for ΔM_d and ΔM_s , it follows that the quantities ΔM_d and ΔM_s are enhanced by the same factor in minimal flavour violation supersymmetry, as compared to their SM values, but the ratio $\Delta M_s / \Delta M_d$ in this theory is the same as in the SM.

The NLO QCD-corrected Hamiltonian for $\Delta S = 2$ transitions in the minimal flavour violation supersymmetric framework has also been obtained in Ref. [58]. From this, the result for ϵ can be written as:

$$|\epsilon| = \frac{G_F^2 f_K^2 M_K M_W^2}{6\sqrt{2}\pi^2 \Delta M_K} \hat{B}_K \left(A^2 \lambda^6 \eta \right) (y_c \{ \hat{\eta}_{ct} f_3(y_c, y_t) - \hat{\eta}_{cc} \} + \hat{\eta}_2(K) S A^2 \lambda^4 (1 - \rho)), \quad (40)$$

where the NLO QCD correction factor is [58]:

$$\hat{\eta}_2(K) = \alpha_s(m_c)^{\gamma^{(0)}/(2\beta_3^{(0)})} \left(\frac{\alpha_s(m_b)}{\alpha_s(m_c)} \right)^{\gamma^{(0)}/(2\beta_4^{(0)})} \left(\frac{\alpha_s(M_W)}{\alpha_s(m_b)} \right)^{\gamma^{(0)}/(2\beta_5^{(0)})} \times \left[1 + \frac{\alpha_s(m_c)}{4\pi} (Z_3 - Z_4) + \frac{\alpha_s(m_b)}{4\pi} (Z_4 - Z_5) + \frac{\alpha_s(M_W)}{4\pi} \left(\frac{D}{S} + Z_5 \right) \right]. \quad (41)$$

Here

$$Z_{n_f} = \frac{\gamma_{n_f}^{(1)}}{2\beta_{n_f}^{(0)}} - \frac{\gamma^{(0)}}{2\beta_{n_f}^{(0)2}} \beta_{n_f}^{(1)}, \quad (42)$$

and the quantities entering in Eqs. (38) and (41) are the coefficients of the well-known beta function and anomalous dimensions in QCD: The ratio

$$\frac{\hat{\eta}_{2,S}(B)(NLO)}{\hat{\eta}_{2,S}(B)(LO)} = 1 + \frac{\alpha_s(M_W)}{4\pi} \left(\frac{D}{S} + Z_5 \right), \quad (43)$$

is worked out numerically in Ref. [58] as a function of the supersymmetric parameters (chargino mass m_{χ_2} , mass of the lighter of the two stops $m_{\tilde{t}_R}$, and the mixing angle ϕ in the stop sector). This ratio is remarkably stable against variations in the mentioned parameters and is found numerically to be about 0.89. Since in the LO approximation the QCD correction factor $\hat{\eta}_{2,S}(B)(LO)$ is the same in the SM and SUSY, the QCD correction factor $\hat{\eta}_{2,S}(B)(NLO)$ entering in the expressions for ΔM_d and ΔM_s in the MSSM is found to be $\hat{\eta}_{2,S}(B)(NLO) = 0.51$ in the \overline{MS} -scheme. This is to be compared with the corresponding quantity $\hat{\eta}_B = 0.55$ in the SM. Thus, NLO corrections in ΔM_d (and ΔM_s) are similar in the SM and MSSM, but not identical.

The expression for $\hat{\eta}_{2,S}(K)(NLO)/\hat{\eta}_{2,S}(K)(LO)$ can be expressed in terms of the ratio $\hat{\eta}_{2,S}(B)(NLO)/\hat{\eta}_{2,S}(B)(LO)$ given above and the flavour-dependent matching factors Z_{n_f} :

$$\begin{aligned} \frac{\hat{\eta}_{2,S}(K)(NLO)}{\hat{\eta}_{2,S}(K)(LO)} &= \frac{\hat{\eta}_{2,S}(B)(NLO)}{\hat{\eta}_{2,S}(B)(LO)} + \frac{\alpha_s(m_c)}{4\pi} (Z_3 - Z_4) + \frac{\alpha_s(m_b)}{4\pi} (Z_4 - Z_5) \\ &\simeq 0.884, \end{aligned} \quad (44)$$

where we have used the numerical value $\hat{\eta}_{2,S}(B)(NLO)/\hat{\eta}_{2,S}(B)(LO) = 0.89$ calculated by Krauss and Soff [58], along with $\alpha_s(m_c) = 0.34$ and $\alpha_s(m_b) = 0.22$. Using the expression for the quantity $\hat{\eta}_{2,S}(K)(LO)$, which is given by the prefactor multiplying the square bracket in Eq. (41), one gets $\hat{\eta}_{2,S}(K)(NLO) = 0.53$ in the \overline{MS} -scheme. This is to be compared with the corresponding QCD correction factor in the SM, $\hat{\eta}_{tt} = 0.57$, given in Table 1. Thus the two NLO factors are again very similar but not identical.

Following the above discussion, the SUSY contributions to ΔM_d , ΔM_s and $|\epsilon|$ in supersymmetric theories are incorporated in our analysis in a simple form:

$$\begin{aligned} \Delta M_d &= \Delta M_d(SM) [1 + f_d(m_{\chi_2^\pm}, m_{\tilde{t}_R}, m_{H^\pm}, \tan v, \phi)], \\ \Delta M_s &= \Delta M_s(SM) [1 + f_s(m_{\chi_2^\pm}, m_{\tilde{t}_R}, m_{H^\pm}, \tan v, \phi)], \\ |\epsilon| &= \frac{G_F^2 f_K^2 M_K M_W^2}{6\sqrt{2}\pi^2 \Delta M_K} \hat{B}_K \left(A^2 \lambda^6 \eta \right) (y_c \{ \hat{\eta}_{ct} f_3(y_c, y_t) - \hat{\eta}_{cc} \} \\ &\quad + \hat{\eta}_{tt} y_t f_2(y_t) [1 + f_\epsilon(m_{\chi_2^\pm}, m_{\tilde{t}_2}, m_{H^\pm}, \tan v, \phi)] A^2 \lambda^4 (1 - \rho)). \end{aligned} \quad (45)$$

Here, ϕ is the LR -mixing angle in the stop sector. The quantities f_d , f_s and f_ϵ can be expressed as

$$f_d = f_s = \frac{\hat{\eta}_{2,S}(B)}{\hat{\eta}_B} R_{\Delta_d}(S) , \quad f_\epsilon = \frac{\hat{\eta}_{2,S}(K)}{\hat{\eta}_{tt}} R_{\Delta_d}(S), \quad (46)$$

where $R_{\Delta_d}(S)$ is defined as

$$R_{\Delta_d}(S) \equiv \frac{\Delta M_d(SUSY)}{\Delta M_d(SM)}(LO) = \frac{S}{y_t f_2(y_t)} . \quad (47)$$

The functions f_i , $i = d, s, \epsilon$ are all positive definite, i.e. the supersymmetric contributions add *constructively* to the SM contributions in the entire allowed supersymmetric parameter space. We find that the two QCD correction factors appearing in Eq. (46) are numerically very close to one another, with $\hat{\eta}_{2,S}(B)/\hat{\eta}_B \simeq \hat{\eta}_{2,S}(K)/\hat{\eta}_{tt} = 0.93$. Thus, to an excellent approximation, one has $f_d = f_s = f_\epsilon \equiv f$.

How big can f be? This quantity is a function of the masses of the top squark, chargino and the charged Higgs, $m_{\tilde{t}_R}$, $m_{\tilde{\chi}_2^\pm}$ and m_{H^\pm} , respectively, as well as of $\tan v$. The maximum allowed value of f depends on the model (minimal SUGRA, non-minimal SUGRA, MSSM with constraints from EDMs, etc.). We have numerically calculated the quantity f by varying the SUSY parameters ϕ , $m_{\tilde{t}_R}$, $m_{\chi_2^\pm}$, m_{H^\pm} and $\tan v$. Using, for the sake of illustration, $m_{\chi_2^\pm} = m_{\tilde{t}_R} = m_{H^\pm} = 100$ GeV, $m_{\chi_1^\pm} = 400$ GeV and $\tan v = 2$, and all other supersymmetric masses much heavier, of $O(1)$ TeV, we find that the quantity f varies in the range:

$$0.4 \leq f \leq 0.8 \quad \text{for} \quad |\phi| \leq \pi/4 , \quad (48)$$

with the maximum value of f being at $\phi = 0$. This is shown in Fig. 7, where we have plotted the function f against ϕ (upper figure), and against $m_{\chi_2^\pm}$, $m_{\tilde{t}_R}$ and m_{H^\pm} (lower figure), varying one parameter at a time and holding the others fixed to their stated values given above. These parametric values are allowed by the constraints from the NLO analysis of the decay $B \rightarrow X_s + \gamma$ reported in Ref. [42], as well as from direct searches of the supersymmetric particles [2]. The allowed value of f decreases as $m_{\tilde{t}_R}$, $m_{\chi_2^\pm}$ and m_{H^\pm} increase, though the dependence of f on m_{H^\pm} is rather mild due to the compensating effect of the H^\pm and chargino contributions in the MSSM, as observed in Ref. [42]. Likewise, the allowed range of f is reduced as $\tan v$ increases, as shown in Fig. 8 for $\tan v = 4$, in which case one has $0.15 \leq f \leq 0.42$ for $|\phi| \leq \pi/4$. This sets the size of f allowed by the present constraints in the minimal flavour violation version of the MSSM.

If additional constraints on the supersymmetry breaking parameters are imposed, as is the case in the minimal and non-minimal versions of the SUGRA models, then the allowed values of f will be further restricted. A complete NLO analysis of f would require a monte-carlo approach implementing all the experimental and theoretical constraints (such as the SUGRA-type mass relations). In particular, the NLO correlation between $B(B \rightarrow X_s \gamma)$ and f has to be studied in an analogous fashion, as has been done, for example, in Refs. [54,55] with the leading order SUSY effects.

In this paper we adopt an approximate method to constrain f in SUGRA-type models. We take the maximum allowed values of the quantity $R_{\Delta_d}(S)$, defined earlier, from the existing LO analysis of the same and obtain f by using Eq. (46). For the sake of definiteness, we use the updated work of Goto et al. [54,55].

From the published results we conclude that typically f can be as large as 0.45 in non-minimal SUGRA models for low $\tan v$ (typically $\tan v = 2$) [54], and approximately half of this value in minimal SUGRA models [46,53,54]. Relaxing the SUGRA mass constraints, admitting complex values of A and μ but incorporating the EDM constraints, and imposing the constraints mentioned above, Baek and Ko [50] find that f could be as large as $f = 0.75$. In all cases, the value of f decreases with increasing $\tan v$ or increasing $m_{\tilde{\chi}_2^\pm}$ and $m_{\tilde{t}_R}$, as noted above.

3.3 SUSY Fits

For the SUSY fits, we use the same program as for the SM fits, except that the theoretical expressions for ΔM_d , ΔM_s and $|\epsilon|$ are modified as in Eq. (45). We compare the fits for four representative values of the SUSY function f — 0, 0.2, 0.4 and 0.75 — which are typical of the SM, minimal SUGRA models, non-minimal SUGRA models, and non-SUGRA models with EDM constraints, respectively.

The allowed 95% C.L. regions for these four values of f are all plotted in Fig. 11. As is clear from this figure, there is still a considerable overlap between the $f = 0$ (SM) and $f = 0.75$ regions. However, there are also regions allowed for one value of f which are excluded for another value. Thus a sufficiently precise determination of the unitarity triangle might be able to exclude certain values of f (including the SM, $f = 0$).

From Fig. 11 it is clear that a measurement of the CP angle β will *not* distinguish among the various values of f : even with the naked eye it is evident that the allowed range for β is roughly the same for all models. Rather, it is the measurement of γ or α which has the potential to rule out certain values of f .

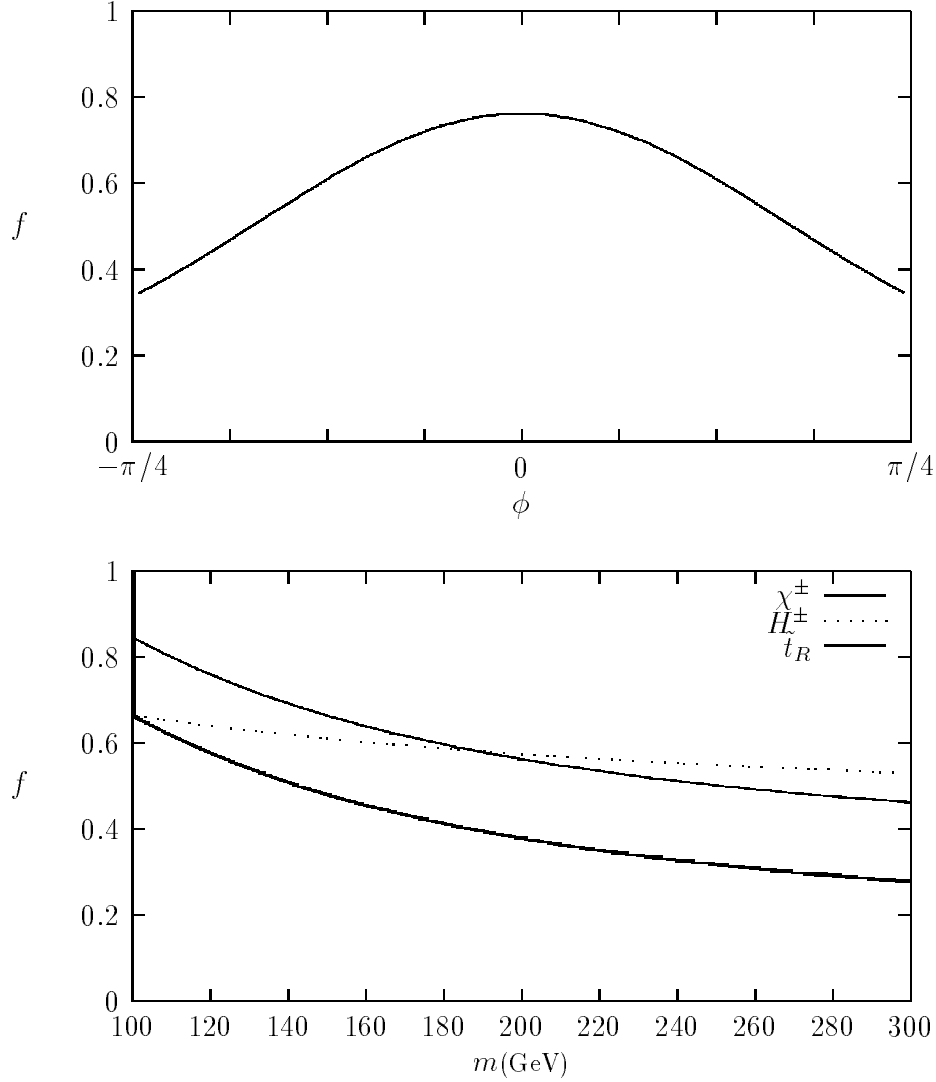


Fig. 7. Dependence of the supersymmetric function f on the LR -mixing angle in the stop sector, ϕ (upper figure), and on $m_{\tilde{\chi}_2^\pm}$, m_{H^\pm} and $m_{\tilde{t}_R}$ (lower figure), for $\tan v = 2$; values of the other supersymmetric parameters are stated in the text.

As f increases, the allowed region moves slightly down and towards the right in the ρ - η plane, corresponding to smaller values of γ (or equivalently, larger values of α). We illustrate this in Table 2, where we present the allowed ranges of α , β and γ , as well as their central values (corresponding to the preferred values of ρ and η), for each of the four values of f . From this Table, we see that the allowed range of β is largely insensitive to the model. Conversely, the allowed values of α and γ do depend somewhat strongly on the chosen value of f . Note, however, that one is not guaranteed to be able to distinguish among the various models: as mentioned above, there is still significant overlap among

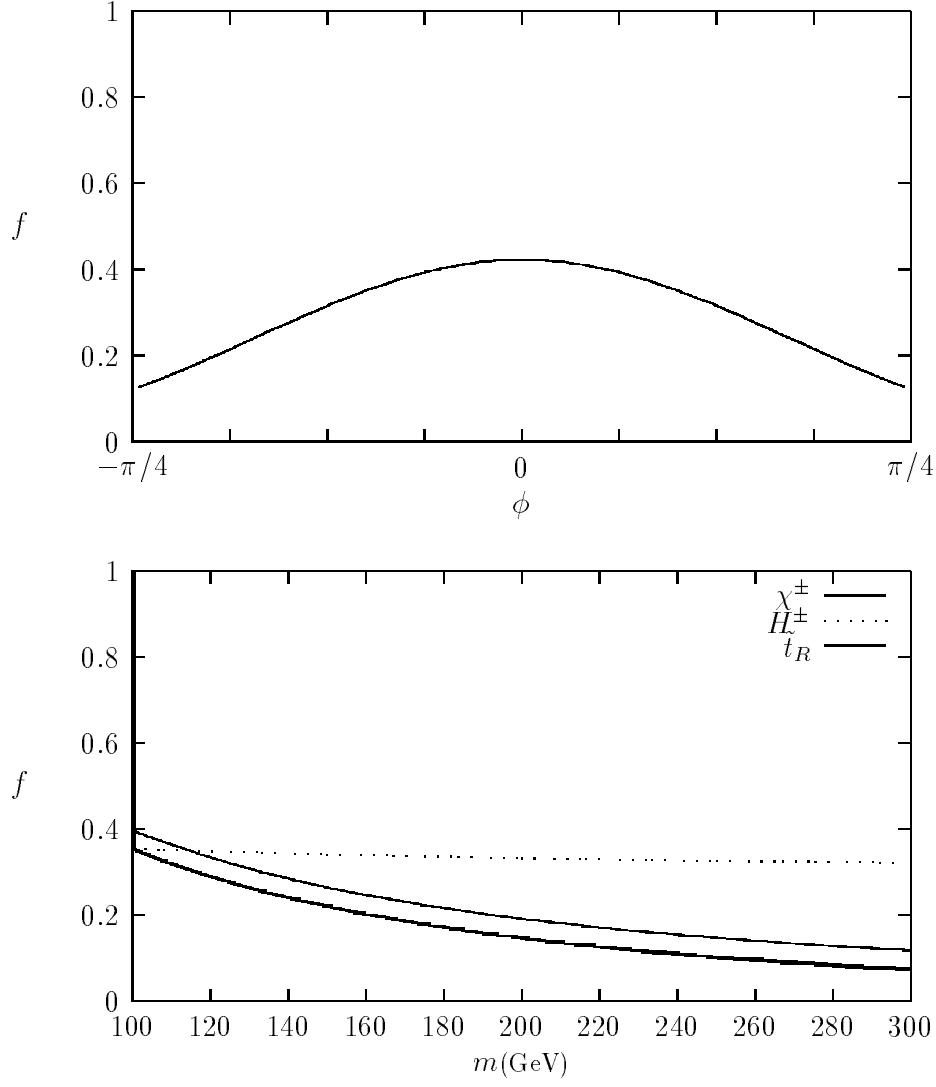


Fig. 8. Dependence of the supersymmetric function f on the LR -mixing angle in the stop sector, ϕ (upper figure), and on $m_{\tilde{\chi}_2^\pm}$, m_{H^\pm} and $m_{\tilde{t}_R}$ (lower figure), for $\tan v = 4$; values of the other supersymmetric parameters are stated in the text.

all four models. Thus, depending on what values of α and γ are obtained, we may or may not be able to rule out certain values of f .

One point which is worth emphasizing is the correlation of γ with f . This study clearly shows that large values of f require smaller values of γ . The reason that this is important is as follows. The allowed range of γ for a particular value of f is obtained from a fit to all CKM data, even those measurements which are unaffected by the presence of supersymmetry. Now, the size of γ indirectly affects the branching ratio for $B \rightarrow X_s \gamma$: a larger value of γ corresponds to

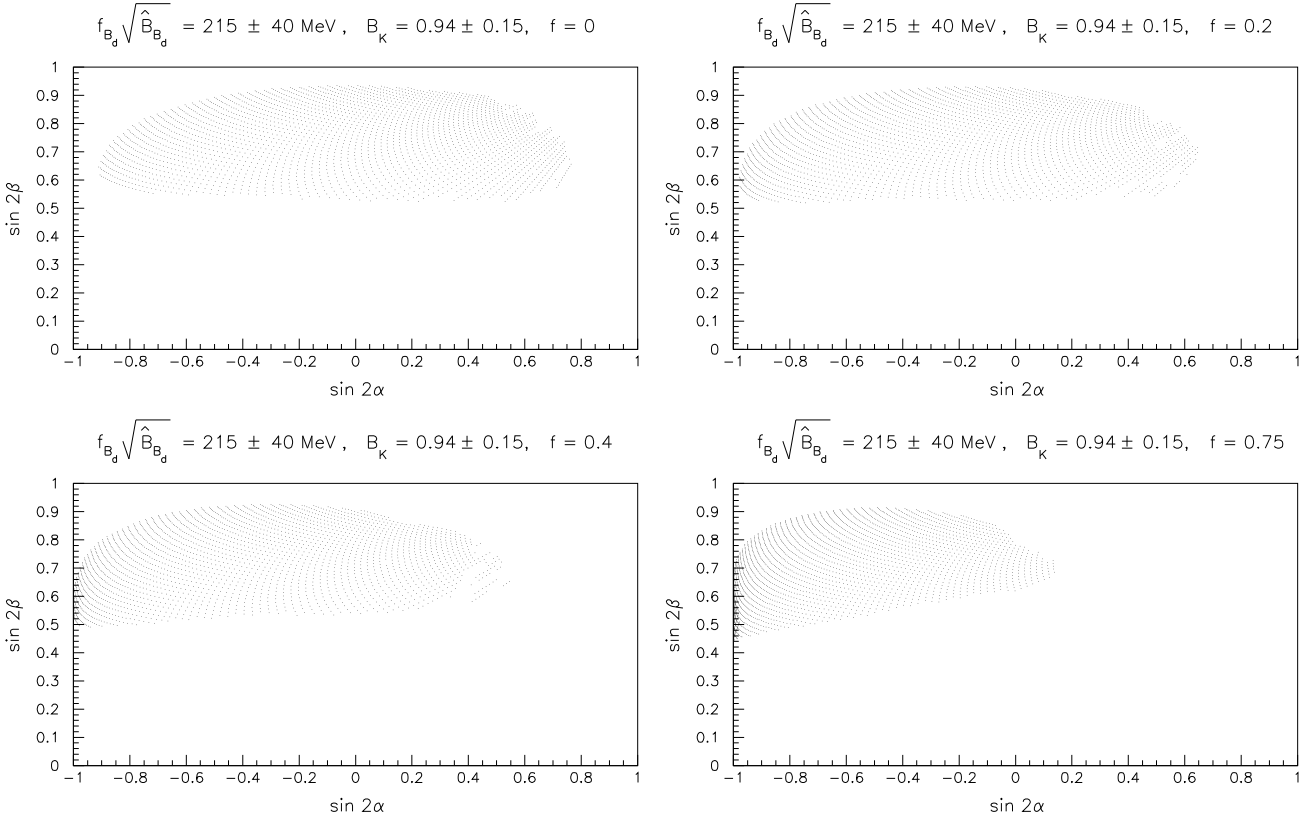


Fig. 9. Allowed 95% C.L. region of the CP-violating quantities $\sin 2\alpha$ and $\sin 2\beta$, from a fit to the data given in Table 1. The upper left plot ($f = 0$) corresponds to the SM, while the other plots ($f = 0.2, 0.4, 0.75$) correspond to various SUSY models. (From Ref. [19].)

f	α	β	γ	$(\alpha, \beta, \gamma)_{\text{cent}}$
$f = 0$ (SM)	$65^\circ - 123^\circ$	$16^\circ - 35^\circ$	$36^\circ - 97^\circ$	$(93^\circ, 25^\circ, 62^\circ)$
$f = 0.2$	$70^\circ - 129^\circ$	$16^\circ - 34^\circ$	$32^\circ - 90^\circ$	$(102^\circ, 24^\circ, 54^\circ)$
$f = 0.4$	$75^\circ - 134^\circ$	$15^\circ - 34^\circ$	$28^\circ - 85^\circ$	$(110^\circ, 23^\circ, 47^\circ)$
$f = 0.75$	$86^\circ - 141^\circ$	$13^\circ - 33^\circ$	$23^\circ - 73^\circ$	$(119^\circ, 22^\circ, 39^\circ)$

Table 2

Allowed 95% C.L. ranges for the CP phases α , β and γ , as well as their central values, from the CKM fits in the SM ($f = 0$) and supersymmetric theories, characterized by the parameter f defined in the text.

a smaller value of $|V_{ts}|$ through CKM unitarity. And this branching ratio is among the experimental data used to bound SUSY parameters and calculate the allowed range of f . Therefore, the above γ - f correlation indirectly affects the allowed values of f in a particular SUSY model, and thus must be taken into account in studies which examine the range of f . For example, it is often the case that larger values of f are allowed for large values of γ . However, as we have seen above, the CKM fits disfavour such values of γ .

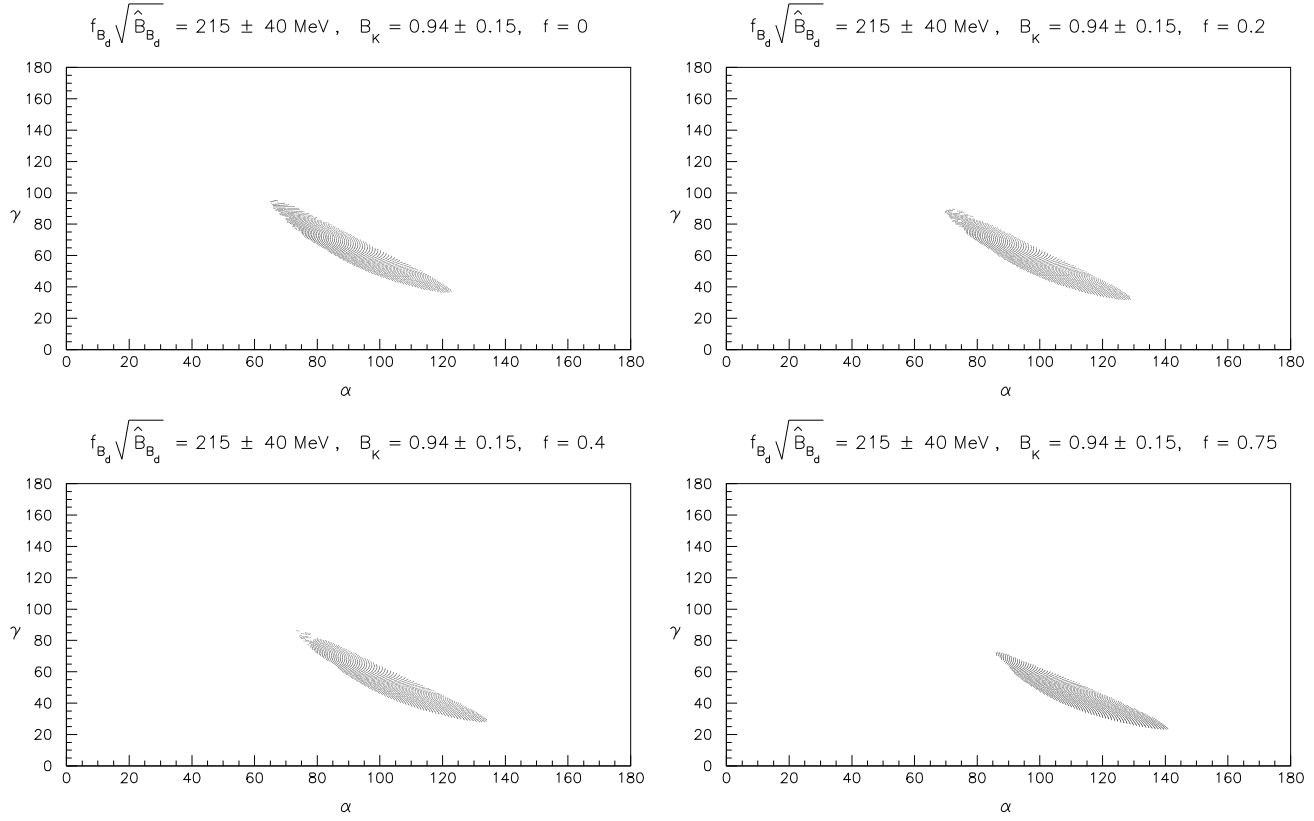


Fig. 10. Allowed 95% C.L. region of the CP-violating quantities α and γ , from a fit to the data given in Table 1. The upper left plot ($f = 0$) corresponds to the SM, while the other plots ($f = 0.2, 0.4, 0.75$) correspond to various SUSY models. (From Ref. [19].)

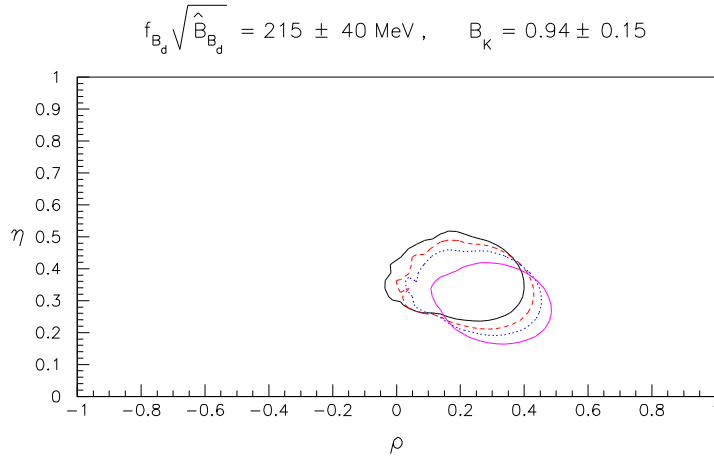


Fig. 11. Allowed 95% C.L. region in ρ - η space in the SM and in SUSY models, from a fit to the data given in Table 1. From left to right, the allowed regions correspond to $f = 0$ (SM, solid line), $f = 0.2$ (long dashed line), $f = 0.4$ (short dashed line), $f = 0.75$ (dotted line). (From Ref. [19].)

f	$\sin 2\alpha$	$\sin 2\beta$	$\sin^2 \gamma$
$f = 0$ (SM)	$-0.91 - 0.77$	$0.53 - 0.94$	$0.35 - 1.00$
$f = 0.2$	$-0.98 - 0.65$	$0.52 - 0.93$	$0.28 - 1.00$
$f = 0.4$	$-1.00 - 0.50$	$0.49 - 0.93$	$0.22 - 0.99$
$f = 0.75$	$-1.00 - 0.14$	$0.45 - 0.91$	$0.16 - 0.91$

Table 3

Allowed 95% C.L. ranges for the CP asymmetries $\sin 2\alpha$, $\sin 2\beta$ and $\sin^2 \gamma$, from the CKM fits in the SM ($f = 0$) and supersymmetric theories, characterized by the parameter f defined in the text.

For completeness, in Table 3 we present the corresponding allowed ranges for the CP asymmetries $\sin 2\alpha$, $\sin 2\beta$ and $\sin^2 \gamma$. Again, we see that the allowed range of $\sin 2\beta$ is largely independent of the value of f . On the other hand, as f increases, the allowed values of $\sin 2\alpha$ become increasingly negative, while those of $\sin^2 \gamma$ become smaller.

The allowed (correlated) values of the CP angles for various values of f can be clearly seen in Figs. 9 and 10. As f increases from 0 (SM) to 0.75, the change in the allowed $\sin 2\alpha$ – $\sin 2\beta$ (Fig. 9) and α – γ (Fig. 10) regions is quite significant.

In Sec. 2.1, we noted that $|V_{ub}/V_{cb}|$, \hat{B}_K and $f_{B_d}\sqrt{\hat{B}_{B_d}}$ are very important in defining the allowed region in the ρ – η plane. At present, these three quantities have large errors, which are mostly theoretical in nature. Let us suppose that our theoretical understanding of these quantities improves, so that the errors are reduced by a factor of two, i.e.

$$\begin{aligned}
\left| \frac{V_{ub}}{V_{cb}} \right| &= 0.093 \pm 0.007, \\
\hat{B}_K &= 0.94 \pm 0.07, \\
f_{B_d}\sqrt{\hat{B}_{B_d}} &= 215 \pm 20 \text{ MeV}.
\end{aligned} \tag{49}$$

How would such an improvement affect the SUSY fits?

We present the allowed 95% C.L. regions ($f = 0, 0.2, 0.4, 0.75$) for this hypothetical situation in Fig. 12. Not surprisingly, the regions are quite a bit smaller than in Fig. 11. More importantly for our purposes, the regions for the different values of f have become more separated from one another. That is, although there is still a region where all four f values are allowed, precise measurements of the CP angles have a better chance of ruling out certain values of f .

In Table 4 we present the allowed ranges of α , β and γ , as well as their central values, for this scenario. Table 5 contains the corresponding allowed ranges for the CP asymmetries $\sin 2\alpha$, $\sin 2\beta$ and $\sin^2 \gamma$. The allowed $\sin 2\alpha$ – $\sin 2\beta$

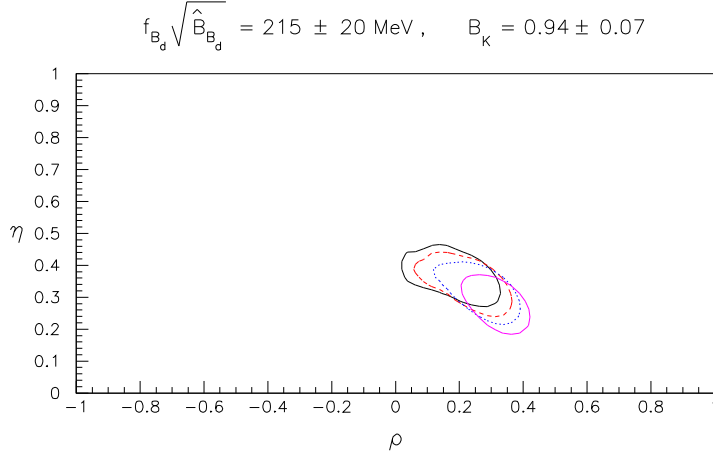


Fig. 12. Allowed 95% C.L. region in ρ - η space in the SM and in SUSY models, from a fit to the data given in Table 1, with the (hypothetical) modifications given in Eq. (49). From left to right, the allowed regions correspond to $f = 0$ (SM, solid line), $f = 0.2$ (long dashed line), $f = 0.4$ (short dashed line), $f = 0.75$ (dotted line). (From Ref. [19].)

and α - γ correlations can be seen in [19]. As is consistent with the smaller regions of Fig. 11, the allowed (correlated) regions are considerably reduced compared to Figs. 9 and 10. As before, although the measurement of β will not distinguish among the various values of f , the measurement of α or γ may.

Indeed, the assumed reduction of errors in Eq. (49) increases the likelihood of this happening. For example, consider again Table 2, which uses the original data set of Table 1. Here we see that $65^\circ \leq \alpha \leq 123^\circ$ for $f = 0$ and $86^\circ \leq \alpha \leq 141^\circ$ for $f = 0.75$. Thus, if experiment finds α in the range 86° – 123° , one cannot distinguish the SM ($f = 0$) from the SUSY model with $f = 0.75$. However, consider now Table 4, obtained using data with reduced errors. Here, $67^\circ \leq \alpha \leq 116^\circ$ for $f = 0$ and $97^\circ \leq \alpha \leq 137^\circ$ for $f = 0.75$. Now, it is only if experiment finds α in the range 97° – 116° that one cannot distinguish $f = 0$ from $f = 0.75$. But this range is quite a bit smaller than that obtained using the original data. This shows how an improvement in the precision of the data can help not only in establishing the presence of new physics, but also in distinguishing among various models of new physics.

4 Conclusions

In the very near future, CP-violating asymmetries in B decays will be measured at B -factories, HERA-B and hadron colliders. Such measurements will give us crucial information about the interior angles α , β and γ of the unitarity triangle. If we are lucky, there will be an inconsistency in the independent

f	α	β	γ	$(\alpha, \beta, \gamma)_{\text{cent}}$
$f = 0$ (SM)	$67^\circ - 116^\circ$	$20^\circ - 30^\circ$	$42^\circ - 90^\circ$	$(93^\circ, 24^\circ, 63^\circ)$
$f = 0.2$	$74^\circ - 124^\circ$	$19^\circ - 29^\circ$	$36^\circ - 82^\circ$	$(102^\circ, 24^\circ, 54^\circ)$
$f = 0.4$	$83^\circ - 130^\circ$	$18^\circ - 29^\circ$	$31^\circ - 73^\circ$	$(110^\circ, 23^\circ, 47^\circ)$
$f = 0.75$	$97^\circ - 137^\circ$	$16^\circ - 28^\circ$	$26^\circ - 59^\circ$	$(119^\circ, 22^\circ, 39^\circ)$

Table 4

Allowed 95% C.L. ranges for the CP phases α , β and γ , as well as their central values, from the CKM fits in the SM ($f = 0$) and supersymmetric theories, characterized by the parameter f defined in the text. We use the data given in Table 1, with the (hypothetical) modifications given in Eq. (49).

f	$\sin 2\alpha$	$\sin 2\beta$	$\sin^2 \gamma$
$f = 0$ (SM)	$-0.80 - 0.71$	$0.64 - 0.86$	$0.44 - 1.00$
$f = 0.2$	$-0.93 - 0.53$	$0.61 - 0.85$	$0.34 - 0.98$
$f = 0.4$	$-0.99 - 0.23$	$0.57 - 0.85$	$0.27 - 0.91$
$f = 0.75$	$-1.00 - -0.23$	$0.52 - 0.83$	$0.19 - 0.73$

Table 5

Allowed 95% C.L. ranges for the CP asymmetries $\sin 2\alpha$, $\sin 2\beta$ and $\sin^2 \gamma$, from the CKM fits in the SM ($f = 0$) and supersymmetric theories, characterized by the parameter f defined in the text. We use the data given in Table 1, with the (hypothetical) modifications given in Eq. (49).

measurements of the sides and angles of this triangle, thereby revealing the presence of new physics.

If present, this new physics will affect B decays principally through new contributions to $B^0-\overline{B}^0$ mixing. If these contributions come with new phases (relative to the SM), then the CP asymmetries can be enormously shifted from their SM values. In this case there can be huge discrepancies between measurements of the angles and the sides, so that the new physics will be easy to find.

A more interesting possibility, from the point of view of making predictions, are models which contribute to $B^0-\overline{B}^0$ mixings and $|\epsilon|$, but without new phases. One type of new physics which does just this is supersymmetry (SUSY). There are some SUSY models which do contain new phases, but they suffer from the problem described above: lack of predictivity. However, there is also a large class of SUSY models with no new phases. In this paper we have concentrated on these models.

In these models, there are new, supersymmetric contributions to $K^0-\overline{K}^0$, $B_d^0-\overline{B}_d^0$ and $B_s^0-\overline{B}_s^0$ mixing. The key ingredient in our analysis is the fact that these contributions, which add constructively to the SM, depend on the SUSY parameters in essentially the same way. That is, so far as an analysis of the unitarity triangle is concerned, there is a single parameter, f , which characterizes the various SUSY models within this class of models ($f = 0$ corresponds to

the SM). For example, the values $f = 0.2, 0.4$ and 0.75 are found in minimal SUGRA models, non-minimal SUGRA models, and non-SUGRA models with EDM constraints, respectively.

We have therefore updated the profile of the unitarity triangle in both the SM and some variants of the MSSM. We have used the latest experimental data on $|V_{cb}|$, $|V_{ub}/V_{cb}|$, ΔM_d and ΔM_s , as well as the latest theoretical estimates (including errors) of \hat{B}_K , $f_{B_d}\sqrt{\hat{B}_{B_d}}$ and $\xi_s \equiv f_{B_d}\sqrt{\hat{B}_{B_d}}/f_{B_s}\sqrt{\hat{B}_{B_s}}$. In addition to $f = 0$ (SM), we considered the three SUSY values of f : $0.2, 0.4$ and 0.75 .

We first considered the profile of the unitarity triangle in the SM, shown in Fig. 2. At present, the allowed ranges for the CP angles at 95% C.L. are

$$65^\circ \leq \alpha \leq 123^\circ, \quad 16^\circ \leq \beta \leq 35^\circ, \quad 36^\circ \leq \gamma \leq 97^\circ, \quad (50)$$

or equivalently,

$$-0.91 \leq \sin 2\alpha \leq 0.77, \quad 0.52 \leq \sin 2\beta \leq 0.94, \quad 0.35 \leq \sin^2 \gamma \leq 1.00. \quad (51)$$

We have also performed CKM fits for the superweak model. This is done by leaving out the constraint from $|\epsilon|$. The resulting allowed unitarity triangle now depends on the value of $f_{B_d}\sqrt{\hat{B}_{B_d}}$. With the present estimate $f_{B_d}\sqrt{\hat{B}_{B_d}} = 215 \pm 40$ MeV, the superweak case, i.e. $\eta = 0$, is ruled out at 95% C.L. However, unless the theoretical error on this quantity is reduced, the resulting value of η has a large uncertainty.

We then compared the SM with the different SUSY models. The result can be seen in Fig. 11. As f increases, the allowed region moves slightly down and to the right in the ρ - η plane. The main conclusion from this analysis is that the measurement of the CP angle β will not distinguish among the SM and the various SUSY models – the allowed region of β is virtually the same in all these models. On the other hand, the allowed ranges of α and γ do depend on the choice of f . For example, larger values of f tend to favour smaller values of γ . Thus, with measurements of γ or α , we may be able to rule out certain values of f (including the SM, $f = 0$). However, we also note that there is no guarantee of this happening – at present there is still a significant region of overlap among all four models.

Finally, we also considered a hypothetical future data set in which the errors on $|V_{ub}/V_{cb}|$, \hat{B}_K and $f_{B_d}\sqrt{\hat{B}_{B_d}}$, which are mainly theoretical, are reduced by a factor of two. For two of these quantities ($|V_{ub}/V_{cb}|$ and $f_{B_d}\sqrt{\hat{B}_{B_d}}$), this has the effect of reducing the uncertainty on the sides of the unitarity triangle by the same factor. The comparison of the SM and SUSY models is shown in Fig. 12. As expected, the allowed regions for all models are quite a bit smaller

than before. Furthermore, the regions for different values of f have become more separated, so that precise measurements of the CP angles have a better chance of ruling out certain values of f .

Acknowledgements

We thank Laksana Tri Handoko for his help in producing Figs. 7 and 8.

References

- [1] L.B. Okun, B.M. Pontecorvo, V.I. Zakharov, *Lett. Nuovo Cim.* **13** (1975) 218.
- [2] C. Caso et al. (Particle Data Group), *Eur. Phys. J.* **C3** (1998) 1.
- [3] N. Cabibbo, *Phys. Rev. Lett.* **10** (1963) 531; M. Kobayashi and K. Maskawa, *Prog. Theor. Phys.* **49** (1973) 652.
- [4] J.F. Donoghue et al., *Phys. Rev.* **D33** (1986) 179; H. Georgi, *Phys. Lett.* **B297** (1992) 353; T. Ohl, G. Ricciardi and E.H. Simmons, *Nucl. Phys.* **403** (1993) 605. See also L. Wolfenstein, *Phys. Lett.* **B164** (1985) 170.
- [5] G. Blaylock, A. Seiden and Y. Nir, *Phys. Lett.* **B355** (1995) 555.
- [6] See, for a review, J.L. Hewett, T. Takeuchi and S. Thomas, preprint SLAC-PUB-7088, hep-ph/9603391.
- [7] A. Ali and C. Jarlskog, *Phys. Lett.* **B144** (1984) 266; A. Ali, B. van Eijk and I. ten Have, *Phys. Lett.* **B189** (1987) 354; *Nucl. Phys.* **292** (1987) 1.
- [8] C. Albajar et al. (UA1 Collaboration), *Phys. Lett.* **B186** (1987) 247; *Erratum ibid* **B197** (1987) 565.
- [9] J. Alexander, in *Proc. of XXIXth. Int. Conf. on High Energy Physics*, Vancouver, B.C., 1998.
- [10] F. Parodi, in *Proc. of XXIXth. Int. Conf. on High Energy Physics*, Vancouver, B.C., 1998.
- [11] A. Ali and Z. Aydin, *Nucl. Phys.* **B148** (1979) 165.
- [12] L. Randall and S. Su, *Nucl. Phys.* **B540** (1999) 37.
- [13] CDF Collaboration, CDF/PUB/BOTTOM/CDF/4855.
- [14] Seminar presented by P. Shawhan (KTEV Collaboration), Fermilab, IL, Feb. 24, 1999; see also <http://fnphyx-www.fnal.gov/experiments/ktev/epsprime/>.
- [15] G.D. Barr et al. (NA31 Collaboration), *Phys. Lett.* **B317** (1993) 233.

- [16] A.J. Buras, preprint TUM-HEP-316-98, hep-ph/9806471.
- [17] S. Adler et al., Phys. Rev. Lett. **79** (1997) 2204.
- [18] M. Narain, in Proc. of the Seventh Int. Symp. on Heavy Flavors, Santa Barbara, Calif., 1997.
- [19] A. Ali and D. London, preprint DESY 99-042, UdeM-GPP-TH-99-58, hep-ph/9903535. (To appear in Eur. Phys. J., C).
- [20] L. Wolfenstein, Phys. Rev. Lett. **51** (1983) 1945.
- [21] For reviews, see, for example, Y. Nir and H. R. Quinn in *B Decays*, edited by S. Stone (World Scientific, Singapore, 1994), p. 362; I. Dunietz, *ibid.*, p. 393; M. Gronau, *Proceedings of Neutrino 94, XVI International Conference on Neutrino Physics and Astrophysics*, Eilat, Israel, May 29 – June 3, 1994, eds. A. Dar, G. Eilam and M. Gronau, Nucl. Phys. (Proc. Suppl.) **B38** (1995) 136.
- [22] A.J. Buras, W. Slominski, and H. Steger, Nucl. Phys. **B238** (1984) 529; *ibid.* **B245** (1984) 369.
- [23] T. Inami and C.S. Lim, Progr. Theor. Phys. **65** (1981) 297.
- [24] S. Herrlich and U. Nierste, Nucl. Phys. **B419** (1994) 292.
- [25] A.J. Buras, M. Jamin and P.H. Weisz, Nucl. Phys. **B347** (1990) 491.
- [26] S. Herrlich and U. Nierste, Phys. Rev. **D52** (1995) 6505.
- [27] T. Draper, preprint hep-lat/9810065 (1998).
- [28] S. Sharpe, preprint hep-lat/9811006 (1998).
- [29] C. Bernard et al., Phys. Rev. Lett. **81** (1998) 4812.
- [30] L. Wolfenstein, Phys. Rev. Lett. **13** (1964) 380.
- [31] A.J. Buras, M. Jamin and M.E. Lautenbacher, Nucl. Phys. **B370** (1992) 69; *ibid.* **B400** (1993) 37; *ibid.* **B400** (1993) 75; *ibid.* **B408** (1993) 209.
- [32] M. Ciuchini et al., Phys. Lett. **B301** (1993) 263; Nucl. Phys. **B415** (1994) 403;
- [33] S. Bertolini, M. Fabbrichesi and J.O. Egg, Nucl. Phys. **B499** (1995) 197; *ibid.* **B476** (1996) 225.
- [34] A.J. Buras and L. Silvestrini, preprint TUM-HEP-334/98, hep-ph/9811471.
- [35] For recent reviews, see R. Gupta, preprint hep-ph/9801412 and L. Conti et al., Phys. Lett. **B421** (1998) 273.
- [36] W.A. Bardeen, A.J. Buras and J.M. Gerard, Phys. Lett. **B180** (1986) 133; Nucl. Phys. **B293** (1987) 787; Phys. Lett. **B192** (1987) 138; G.O. Köhler et al., Phys. Rev. **D58** (1998) 014017.
- [37] H.G. Moser and A. Roussarie, Nucl. Instr. Meth. **A384** (1997) 491.

- [38] S. Mele, preprint CERN-EP/98-133, hep-ph/9810333 (1998).
- [39] F. Parodi, P. Roudeau and A. Stocchi, preprint LAL 98-49, hep-ph/9802289; preprint LAL 99-03, DELPHI 99-27 CONF 226, hep-ex/9903063.
- [40] See, for example, H.P. Nilles, Phys. Rep. **110** (1984) 1.
- [41] A. Masiero and L. Silvestrini, preprint TUM-HEP-303-97, hep-ph/9711401.
- [42] M. Ciuchini, G. Degrassi, P. Gambino and G.F. Giudice, Nucl. Phys. **B534** (1998) 3.
- [43] M. Dugan, B. Grinstein and L.J. Hall, Nucl. Phys. **B255** (1985) 413; S. Dimopoulos and S. Thomas, Nucl. Phys. **B465** (1996) 23.
- [44] A.G. Cohen, D.B. Kaplan and A.E. Nelson, Phys. Lett. **B388** (1996) 588; A.G. Cohen, D.B. Kaplan, F. Lepeintre and A.E. Nelson, Phys. Rev. Lett. **78** (1997) 2300.
- [45] T. Falk, K.A. Olive and M. Srednicki, Phys. Lett. **B354** (1995) 99; T. Falk and K.A. Olive, *ibid.* **B375** (1996) 196.
- [46] T. Nihei, Prog. Theor. Phys. **98** (1997) 1157.
- [47] G.C. Branco, G.C. Cho, Y. Kizukuri and N. Oshimo, Phys. Lett. **B337** (1994) 316; Nucl. Phys. **B449** (1995) 483.
- [48] R. Contino and I. Scimemi, preprint ROME1-1216-98, hep-ph/9809437.
- [49] D.A. Demir, A. Masiero and O. Vives, Phys. Rev. Lett. **82** (1999) 2447.
- [50] S. Baek and P. Ko, preprint KAIST-20/98, SNUTP 98-139, hep-ph/9812229.
- [51] D. Chang, W.-Y. Keung and A. Pilaftsis, Phys. Rev. Lett. **82** (1999) 900.
- [52] T. Goto, T. Nihei and Y. Okada, Phys. Rev. **D53** (1996) 5233.
- [53] T. Goto, Y. Okada, Y. Shimizu and M. Tanaka, Phys. Rev. **D55** (1997) 4273.
- [54] T. Goto, Y. Okada and Y. Shimizu, Phys. Rev. **D58**: 094006 (1998); KEK-TH-611 (1999) (in preparation).
- [55] T. Goto et al., preprint KEK-TH-608, KEK Preprint 98-206, hep-ph/9812369.
- [56] S. Bertolini, F. Borzumati, A. Masiero and G. Ridolphi, Nucl. Phys. **B353** (1991) 591.
- [57] M. Dine and A.E. Nelson, Phys. Rev. **D48** (1993) 1277; M. Dine, A.E. Nelson and Y. Shirman, Phys. Rev. **D51** (1995) 1362; M. Dine, A.E. Nelson, Y. Nir and Y. Shirman, Phys. Rev. **D53** (1996) 2658.
- [58] F. Krauss and G. Soff, preprint hep-ph/9807238.